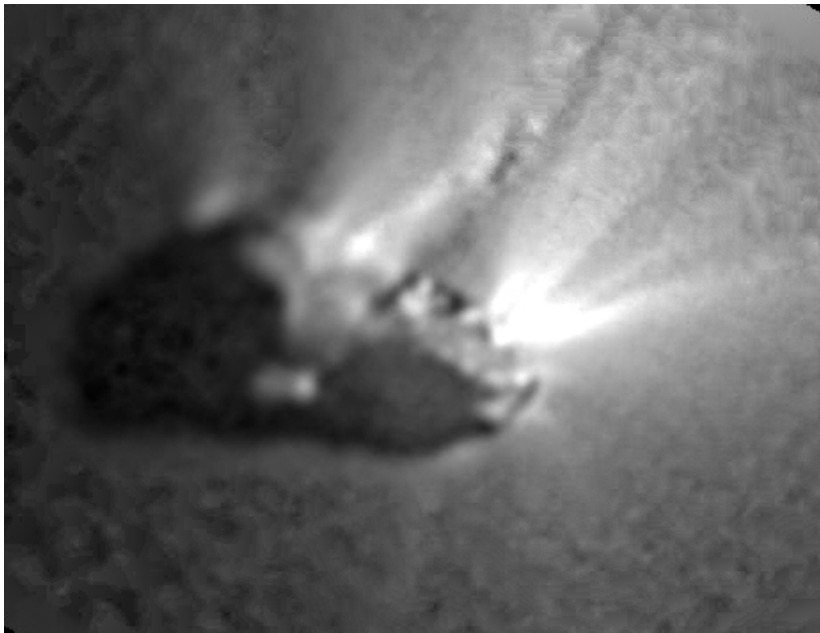
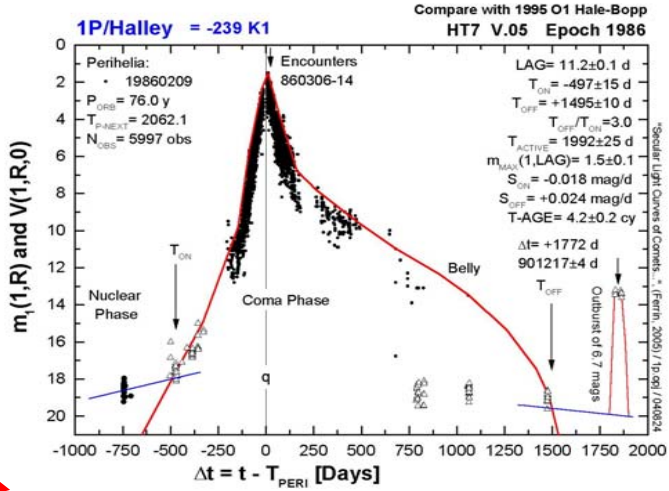
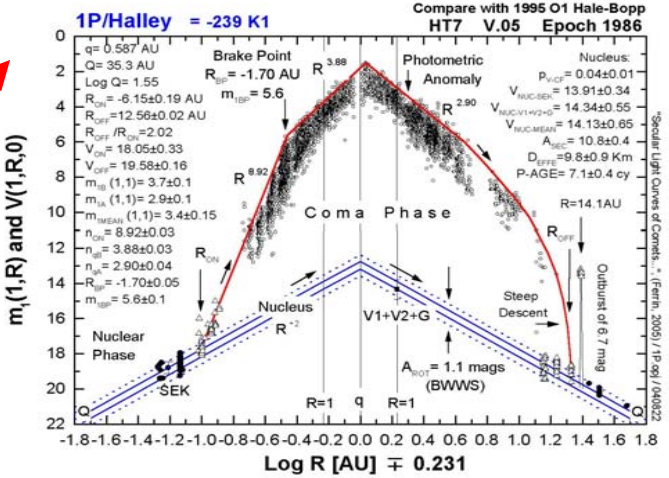
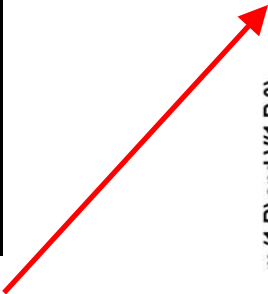


**"ATLAS OF SECULAR LIGHT CURVES OF COMETS, V.2008"**  
**Ignacio Ferrín**



1986, March 14th. Comet 1P/Halley imaged by the Giotto spacecraft. Photo courtesy H. Uwe Keller, Max-Planck Institute für Aeronomie, Lindau, FRG.



F:\Atlas081\Atlas08ConV3.doc / V2008 / 080605

Submitted for publication

# "ATLAS OF SECULAR LIGHT CURVES OF COMETS"

Ignacio Ferrín,  
Center for Fundamental Physics and  
Department of Physics,  
University of the Andes,  
Mérida, Venezuela  
ferrin@ula.ve

Submitted April 03, 2008      Accepted \_\_\_\_\_

Number of Pages: 106  
Number of Figures: 68  
Number of Tables: 4

\* This work contains observations carried out at the National Observatory of Venezuela (ONV), managed by the Center for Research in Astronomy (CIDA), for the Ministry of Science and Technology (MinCyT).

Proposed running head:

"Atlas of Secular Light Curves of Comets "

Ignacio Ferrín,  
Apartado 700,  
Mérida, 5101-A,  
Venezuela,  
South América

ferrin@ula.ve

## Abstract

In this work we have compiled 37.686 observations of 27 periodic and non-periodic comets to create the secular light curves (SLCs), using 2 plots per comet. The data has been reduced homogeneously. Our overriding goal is to learn the properties of the ensemble of comets. More than 40 parameters are listed, of which over 20 are new and measured from the plots. We define two ages for a comet using activity as a proxy, the photometric age P-AGE, and the time-age, T-AGE. It is shown that these two parameters are robust, implying that the input data can have significant errors but P-AGE and T-AGE come out with small errors. This is due to their mathematical definition. It is shown that P-AGE classifies comets by

shape of their light curve. Each SLC can be considered a *fingerprint* of the comet. The value of this Atlas is twofold: The SLCs not only show what we know, but also show what we do not know, thus pointing the way to meaningful observations. Besides their scientific value, these plots are useful for planning observations. The SLCs have not been modeled, and there is no cometary standard thermal model as there is for asteroids. Comets are classified by size and age. In this way it is found that 29P/Schwassmann-Wachmann 1 is a baby goliath comet, while C/1983 J1 Sugano-Saigusa-Fujikawa is a middle age dwarf. There are new classes of comets based on their photometric properties. The secular light curves presented in this Atlas exhibit complexity beyond current understanding.

## 1. Introduction

The comets that populate the solar system represents a fossil record of the formation of our planetary system, and are a valuable tracer of our SS structure and dynamics. Comets are interesting astronomical objects not only from the point of view of their physical properties, but also for their contribution to the interplanetary medium, to our own planet through collisions, and the possibility of having been carriers of water and/or primordial life. Thus the study, analysis and correlations of their properties, including their initial and end states, can yield fundamental clues needed to understand the history of the formation of our SS and their origin and evolution in the sun's gravitational and radiation field.

The system of comets may look distant, faint, cold and uneventful, lurking into the emptiness and darkness of space. However the picture that emerges after looking at the secular light curves (SLCs) presented in this work, is that they are active, complex, eventful, predictable at times, unpredictable at other times, inhomogeneous, and each one has a different personality tied to its composition, age and physical properties. In fact *the SLC can be taken as a fingerprint* of the comet because there are not two identical.

*The value of this Atlas is twofold: The SLCs not only show what we know, but also show what we do not know, thus pointing the way to meaningful observations.* Thus besides their scientific value, the SLCs are very useful for planning observations.

The other value of this Atlas is that it combines nuclear and whole coma magnitudes, thus creating the photometric history of the object. Whole coma magnitudes are determined mostly by amateurs, while faint nuclear magnitudes are measured mostly by professional astronomers. Thus the SLCs successfully combine the work of professionals and amateurs.

It is an illuminating experience to place A4 copies side by side to create a mega-plot, and this exercise is enhanced if they are organized by increasing photometric age, P-AGE. We can then see the richness of shapes, the information and the complexity that the secular light curves exhibit. It is important to realize that the variety of these shapes does not have as of now a theoretical explanation. In this regard we are much farther behind than the corresponding field of variable stars where many of them already have complex theoretical models capable of explaining and extracting numerous physical parameters of the stars, solely from their light curves. Just consider the amount of information derived from RR Lyre, Cepheids and eclipsing binary stars. It is hoped that the present work will help to achieve this goal for comets.

Modeling these SLCs with their different morphologies, is a challenge. The observed SLCs are the sum of light given off by gas and dust, thus really needing two models. Comparing with the field of asteroidal research, we can say that currently *there is no standard thermal model* of cometary secular light curves.

The SLCs are so precisely known in some cases, that there is very little margin of error for fitting theoretical parameters. The ones that come to mind are visual geometric albedo, infrared albedo, bond albedo, thermal conductivity, thickness of the crust layer, pole orientation (obliquity of the nucleus and longitude of the pole), ice composition, and stratigraphic distribution of ices.

At the present moment the Atlas is not complete and work is in progress. In fact, the Atlas will never be completed, because new comets are appearing all the time.

We will present the observational evidence with a minimum of interpretation. Statistical analysis, correlations and ensemble properties will be presented elsewhere.

An explanation of the objectives and methodology of this project has previously been given in Papers I, II, III, IV and V (Ferrín, 2005a, 2005b, 2006, 2007, 2008). The secular light curves previously published are included in the present compilation for reasons of completeness and because some of them have been updated or corrected.

In the above series of papers the approach we used to analyze a comet, was to include all the observations available in the literature. Although this approach gives the maximum amount of information about the objects, it is slow and time consuming. In science, some times another approach is more

convenient. The Version.1 plots presented in this Atlas are not as sophisticated as the Version.Year plots, but nevertheless provide some fundamental information on the object, as the distances of turn on and turn off ( $R_{ON}$ ,  $R_{OFF}$ ), the lag at perihelion, LAG, the photometric age, P-AGE, and the general shape of the SLC. There are several advantages to this second approach: 1) There will be enough objects to make statistical analysis of the comet population. Ensemble properties can be assessed. 2) We get a bird's eye view of the shape of the SLCs. In this work we have adopted this second approach.

## 2. The plots

The magnitude at  $\Delta$ ,  $R$ ,  $\alpha$ , is denoted by  $m_1(\Delta, R)$  for visual observations and  $V(\Delta, R, \alpha)$  for instrumental magnitudes, where  $\Delta$  is the comet-Earth distance,  $R$  is the Sun-comet distance, and  $\alpha$  is the phase angle (comet-Sun-Earth). The information on the brightness of the comet is presented in two plots, the log plot and the time plot. The reason to select the two plots is because they give independent and different parameters. The log plot may be reflected at  $R=1$  AU or may be reflected at  $q$ , the perihelion distance:

1) The "reflected double-log plot" presents the reduced magnitude vs  $\log R$  reflected at  $R=1$  AU. Reduced means reduced to  $\Delta = 1$  AU,  $m(1, R) = m(\Delta, R) - 5 \log \Delta$ . In this plot time runs horizontally from left to right, although non linearly. Negative logs indicate observations pre-perihelion. *The value of the reflected*

*double-log diagram is that power laws on  $R$  ( $R^{+n}$ ) plot as straight lines. Additionally the inclusion of the  $R=1$  AU line allows the determination of the absolute magnitude by extrapolation (actually by interpolation of the pre and post-perihelion intervals).*

It will be shown that the determination of the absolute magnitude of the nucleus, is not always a simple matter as has been assumed in the past. Thus previous determinations of absolute magnitudes should be revised, especially if they are based on the H10 system (see section below on photometry).

**2)** The "time plot" presents the reduced magnitude vs time to perihelion. This is the most basic and simple plot. Negative times are pre-perihelion. The advantage of this plot is that time runs horizontally linearly from left to right thus showing the time history of the object.

**3)** The third type of plot is a "reflected at  $q$ , double-log plot". Comets with extreme LAG values only plot well in the reflected at  $q$  diagram. As a consequence it is not a simple matter to determine the absolute magnitude  $m(1,1)$ . Comet 101P had to be presented with this plot because of its extreme LAG value that distorts the normal log plot reflected at  $R=1$  AU. Also, comets with  $q < 1$  AU have to be presented with this type of plot to make space for the observations inside the Earth's orbit.

The three plots give an unprecedented amount of information on the population of comets, and allow the

elaboration of statistics. Much of this information was not previously available.

The fits to the envelopes and determination of parameters of the secular light curves in general, are my best assessment of the situation. However the reader might choose to apply his own fittings and assessments or re-determine some values of parameters or plot his own observations. This author's interpretation of the SLCs can be found in Section 7.

### **3. Photometric System**

In this section we will describe the methods and mathematical functions and procedures that we have adopted to analyze these data.

#### **3.1 Old H10 Photometric System**

In the old literature the brightness of a comet was defined using the law

$$H = H_0 + 5 \text{ Log } \Delta + 2.5 n \text{ Log } R \quad (1)$$

where  $n$  is a parameter that describes the dependence of the brightness with heliocentric distance, and  $H_0$  is the absolute magnitude at  $\Delta = R = 1$ . The old photometric system H10 assumed  $n = 4$  (Vsekhsvyatskii, 1964).

From the shapes of the secular light curves presented in this work, it is clear that most comets do not

follow power laws, and the 6 that do differ from the  $n = 4$  value used in the H10 system (see Table 1). The other comets exhibit complex secular light curves that have to be defined by more complex laws or even polynomials. In summary we have to conclude that the H10 system, is unable to explain the observed secular light curves. Thus all previous values based on this system should be revised.

### 3.2 Envelope

A visual observation of a comet is affected by several effects, all of which decrease the brightness of the object: moon light, twilight, haze, cirrus clouds, dirty optics, excess magnification, the delta effect, etc. All of these wash out the outer regions of the comet, decreasing its intensity and thus its magnitude. The Delta effect (Kamel, 1997) is produced when a comet gets very near to the Earth. Then our planet may be immersed in the outer regions of the coma. The coma extends out so much in space, that it is impossible to derive a reliable total magnitude. Again some light is left out, decreasing the observed magnitude. *Thus it is a fundamental premise of this work that the envelope of the observations defines the secular light curve, since there is no known physical effect that could increase the perceived brightness of a comet.* It is significant to point out, that even CCD observation may suffer from this complication. If the exposure is not deep enough, the outer parts of the coma will not be recorded, again resulting in an incomplete magnitude.

If as in the past the mean values were used, they would create a significant systematic error of 2-4 magnitudes. Thus previous absolute magnitude determinations have to be revised *upwards*.

Kamel's (1992) compilation on photometric data of comets, included numerical corrections for several effects. In a review of Kamel's work, Green (1991) cites the opinion of Morris on some of his reduction procedures, and concludes that some observation had corrections of 2-6 magnitudes. What is the scientific value of a correction of 6 magnitudes? Since our target error is  $\sim 0.1$  magnitudes, we decided to use only uncorrected magnitudes compiled by Kamel, and let the brightest observations define the envelope. Corrections of the data are not needed if several apparitions are combined. In a given apparition the object may be too low in the sky thus making all the observations systematically low, and thus requiring of an uncertain correction. These same circumstances will not be repeated in the next apparition, and the new observations will be above the old ones defining a nice envelope of the points. Most of the light curves presented in this work are the combination of several apparitions and thus do not require of corrections.

### 3.3 Conversion from $m_1$ to V

$m_1$  observations are mostly taken by amateurs using the naked eye and results are published in the ICQ (International Comet Quarterly, Green, 2007), while V magnitudes are measured by professional astronomers

using CCDs and published in other journals. Ferrín (2005b) has studied this problem and found that the mean conversion from  $m_1$  to V for three comets (1P/Halley, 2P/Encke and C/1973 XII Kohoutek) is  $V = m_1 - 0.026 \pm 0.008$  mag. This value is so small that we will take the two systems as identical.

### 3.4 Conversion from R to V

Corrections due to band passes are still needed, however. Many nuclear magnitudes are measured in R photometric system, and they must be reduced to the V system. In paper II we have compiled a table of V, R and I magnitudes for several comets and we find that the mean  $\langle V-R \rangle$  correction is  $\langle V-R \rangle = 0.48 \pm 0.13$  mag (mean of 77 observations).

### 3.5 Infinite aperture magnitudes

Many observed comets exhibit a prominent coma, so no nuclear magnitude can be derived. Instead, *infinite aperture magnitudes* have to be measured (Ferrín, 2005b).

It has been known for some time (Green, 1997) that there is a lack of flux in many CCD observations. The reasons for this lack of flux was not always clear. Fink et al. (1999) have considered this problem and have found an explanation: *"It is rather well known that visual observations in general, are several magnitudes brighter than CCD measurements and reconciling CCD visual magnitudes is "more of an art than a science".*

*Figure 4 [of their work] shows why this is the case. As we increase the aperture size on our CCD images we get brighter magnitudes. It is evident by the progression of magnitudes for increasing aperture size that if we integrate farther out we would readily reach the magnitudes reported by visual observers. The eye is essentially a logarithmic detector and has a larger dynamic range than a CCD so that it effectively includes more of the coma than an individual non-saturated CCD exposure".*

To avoid this *insufficient CCD aperture error* (Ferrín, 2005b) we have to measure all the light from the comet, *including the tail*. The problem can be illustrated looking at Figure 1 where we show an image of comet 103P/Hartley 2 with a normal stretching of the image, and with a forced stretching. Since large photometric apertures have to be used to extract the whole flux, the image has previously been cleaned of nearby stars, using a background cloning tool.

Stretching refers to the maximum and minimum pixel intensity to display the image in the computer monitor. The normal stretching is selected by the computer, who does not know about preserving the flux. The computer monitor displays a *deceivingly faint* image. It turns out that a forced stretching reveals a much larger tail than expected.

Figure 1 reveals that it is all too common to use photometric CCD apertures that do not extract the whole

flux from the comet producing measurements that lie much below the envelope of the observations.

Of course the optimal extraction aperture increases with the brightness of the comet. We see that a comet of magnitude 16.6 requires an aperture of 2 arc minutes in diameter. Ferrín (2005b) shows that a comet of magnitude 13.3 requires an aperture of 5 arc minutes in diameter. Brighter comets will require even larger apertures.

In Figure 2 we show the method we used to extract an infinite aperture magnitude, IAM, from now on denoted as  $R_{IAM}$ ,  $V_{IAM}$ . The flux is measured with increasing CCD photometric apertures, and *the asymptotic value at infinity is the infinite aperture magnitude*. Usually an exponential fits the data.

Notice how the calibration star #14 converges very rapidly to an infinite aperture magnitude. Not so the comet, that requires an aperture with more than 40 pixels in radius to extract a total flux. Since the scale of this telescope is  $\sim 1''/\text{pixel}$ , 40 pixels represent  $80''$  of diameter =  $1.33'$  of diameter, clearly much larger than the usual apertures published in the literature to extract total magnitudes.

Infinite aperture magnitudes should be adopted whenever the comet exhibits a coma *and tail*. IAM are used in several comets of this *Atlas* and should be adopted by all observers from now on to secure extracting the whole flux of the comet.

### 3.6 Reduction Procedures

In the reduction we must distinguish between the coma observations, and the nucleus observations. The observed visual magnitude of a comet with coma,  $m_1(\Delta, R)$  is given by

$$m_1(\Delta, R) = m(1, 1) + 5 \text{ Log } \Delta + 2.5 n \text{ Log } R \quad (2)$$

where  $m(1, 1)$  is the absolute magnitude of the comet at  $\Delta = 1 \text{ AU}$  and  $R = 1 \text{ AU}$ . The  $\Delta$  correction is a purely geometric parameter due solely to the changing distance Earth-comet, that must be subtracted.

$$m_1(1, R) = m_1(\Delta, R) - 5 \text{ Log } \Delta \quad (3)$$

For nuclear observations an additional term is needed because we are then seeing the bare nucleus under different phase angles:

$$V_N(1, R, \alpha) = V_N(1, 1, 0) + 5 \log \Delta + 5 \text{ Log } R + \beta \cdot \alpha \quad (4)$$

where  $V_N(1, 1, 0)$  is the absolute nuclear magnitude,  $\beta$  is the phase coefficient, and  $\alpha$  the phase angle (earth-comet-Sun). Then

$$V_N(1, R, 0) = V_N(1, 1, 0) - 5 \log \Delta - \beta \cdot \alpha \quad (5)$$

$m_1(1, R)$  and  $V_N(1, R, 0)$  are plotted vs heliocentric distance,  $R$ , in the log plot, and vs time in the time plot.

### 3.7 Rotational error

Most comets have highly elongated nuclei and thus have rotational light curves of large amplitude,  $A_{\text{ROT}}$ , reaching to 1.1 magnitudes in the case of comet 1P/Halley (Belton et al., 1986) which may represent an extreme. Thus snapshot observations are affected by the “rotational error”. We have assigned to snapshot observations a mean error of  $\pm 0.63$  magnitudes to take into account this effect.  $\pm 0.63$  mag represents the 68% percentile of 32 rotational light curve amplitudes.

### 3.8 Photographic measurements

We do not use photographic measurements, and some remaining from Kamel’s (1992) compilation have been deleted. The only exceptions is when there are not enough visual observations (example, 28P/Neujmin). The reason for not using photographic magnitudes is that they are contaminated by the CN line at 3883 Å which is the most intense line of the whole cometary spectrum.

### 3.9 Phase curve, phase coefficient, and absolute nucleus dimensions

The best way to derive the absolute nuclear magnitude of a comet is by plotting the phase diagram,  $V(1,1,\alpha)$  vs  $\alpha$ . The slope of this curve gives the phase coefficient,  $\beta$ , which is needed to reduce nuclear observations to a common phase angle of  $0^\circ$ , and the interception of this line with the y-axis gives  $V_N(1,1,0)$ .

### 3.10 Data sets

We will use the data set of Kamel (1992) without corrections for observations prior to 1990, and the ICQ (Green, 2007) for observations after that date. Many other visual and CCD observations can be found in web sites scattered all around the world. Faint and nuclear observations are compiled from the literature. Many scientific references give nuclear diameters for comets. These values can be converted to absolute magnitude using equations (12) and (13) and assuming a geometric albedo  $p_V = 0.04$ . Particularly useful are the compilations of magnitudes and/or diameters of Chen and Jewitt (1994), Scotti (1995), Lowry et al. (1999), Tancredi et al. (2000, 2006), Neslusan (2003), Lowry and Weissman (2003), Lowry et al. (2003), Meech et al. (2004), Lamy et al. (2005), Lowry and Fitzsimmons (2005), Hicks et al. (2007).

### 3.11 Data prior to 1950

Tom Gehrels (1999) had something relevant to say about former asteroidal photometry (equally valid for cometary photometry): *“Before the 50s, asteroid magnitudes were not usable for statistics. They would be off by as much as 3 magnitudes: fainter than the 11<sup>th</sup> magnitude, they tended to be all the same because the Bonner Durchmusterung had been used for calibration and it did not go fainter”*. Consequently, it is not advisable to use faint observations before the 50s. However there are several cases in which we do not have any other choice.

### 3.12 Absolute Calibration

P-AGE and T-AGE are given in comet years to emphasize that they are not calibrated in Earth's years. Thus there is a need for an absolute calibration. At the present time it is possible to calibrate only comet 2P/Encke in current years (Ferrín, 2008), using the fact that its SLC has been obtained for the Epochs 1858 and 2003. A plot of Earth's years vs P-AGE and T-AGE using a linear extrapolation shows that the comet had P-AGE=0 and T-AGE=0 in  $1640 \pm 100$ . This is not the birth date of the comet but the "effective" date at which the comet began sublimating. However the interpretation and implications of this zero-age-date is much more complex that can be analyzed here and is beyond the scope of this paper. The important point to emphasize is that an absolute calibration *can be achieved*.

## 4. Parameters Measured from the Plots

The two plots provide a wealth of information. There are ~40 parameters listed, of which ~20 are new and measured from the plots.

### 4.1 Log plots

The title of each plot identifies the comet in the new and old system to allow going back to historical references. The first designation of the comet gives the first apparition (the discovery year). The labels JF, SF, OC, ABC, ET, CEN, HT indicate the family, if the comet

belongs to the Jupiter family, to the Saturn family, to the Oort Cloud, to the Asteroidal Belt, to the Encke type, if it is a Centaur or if it belongs to the Halley type. This classification follows closely the one given by Levison (1996), except that Chiron type and Centaur are synonymous, ABC is included in his ecliptic comets and finally he did not consider the existence of Saturn family comets (28P, 85P). The two numbers following the family are the photometric age, P-AGE and the diameter in km. The reason for using P-AGE as a label here is that the definition of P-AGE is robust, as will be demonstrated later on. When reading these numbers it is important to keep in mind that ~95% of comets have  $0 < \text{P-AGE} < 100$  cy and  $0 < D_{\text{EFFE}} < 10$  km. *Any object above 100/10 or near 0/0 is exceptional.*

Next is the Version of the plot. Although most plots have gone through many versions in the course of arriving at a final solution (usually more than 10 versions), all plots are identified as Version 1 (if they are preliminary) or V.08 (the year of publication). The upper left hand side of each plot gives the perihelion distance,  $q$ , the aphelion distance for that epoch,  $Q$  (where  $Q = q(1+e)/(1-e)$  where  $e$  is the eccentricity), and  $\text{Log } Q$  to identify the extent of the plot.  $Q$  and  $q$  can be located at the bottom of the plots and come in units of AU. At the extreme lower right of the plots, the date line tilted  $90^\circ$  is the last update of observations.

The Epoch label identifies the apparition that has contributed most significantly to the definition of the envelope. The importance of this label is that future

apparitions will be plotted in a new Epoch plot, to be compared with the former one. After many apparitions, a movie of the secular light curve could be built with the individual plots, showing evolutionary changes and actually, the photometric history of the comet. Each plot of this Atlas is a frame of that movie.

The following parameters are deduced from the log plots. See Figure 3 for a graphical explanation of these parameters.

**1)  $R_{ON}$  [AU].** The turn-on distance of the coma. The negative sign in this parameter, in  $T_{ON}$  and in Log R in the plots indicates values before perihelion. Physically  $R_{ON}$  corresponds to the onset of *steady* activity. It is the interception of the nuclear line and the coma envelope. Browsing the secular light curves it can be seen that the turn-on and turn-off points are very sudden affairs. When there are enough data points these parameters can be measured easily and accurately because of the sharp change of slope. Usually  $R_{ON}$  takes place *before* perihelion, but for comet 133P/Elst-Pizarro takes place *after* perihelion.

**2)  $R_{OFF}$ .** The turn-off distance of the coma, usually larger than  $R_{ON}$ . This is the interception of the coma envelope and the nuclear line post-perihelion.  $R_{OFF}$  takes place *after* perihelion.

**3)  $R_{SUM} = -R_{ON} + R_{OFF}$ .** This is equivalent to the  $T_{ACTIVE} = -T_{ON} + T_{OFF}$  parameter defined in the time domain. It is a measure of activity.

**4)  $V_{ON}$ .** The magnitude at which the nucleus turns on.

**5)  $V_{OFF}$ .** The magnitude at which the nucleus turns off.

**6)  $-R_{OFF} / R_{ON}$ .** An asymmetry parameter for the log plot.

**7)  $m_{1B}(1,1)$ .** The absolute magnitude of the coma, measured *before* perihelion by extrapolation to Log R = 0. This and the next parameter are needed for comets with  $q < 1$  AU.

**8)  $m_{1A}(1,1)$ ,** the absolute magnitude of the coma *after* perihelion. When the secular light curve is highly asymmetric, the absolute magnitude after perihelion is different from the value before perihelion. In this work the mean value of variable x will be denoted by  $\langle x \rangle$ . Thus  $\langle m_1(1,1) \rangle$  = the mean value of the absolute magnitude before and after perihelion, is used frequently.

**9)  $V_N(1,1,0) = V_{NUC}$ .** Absolute nuclear magnitude measured by different authors. The authors are listed in the individual comments of each comet.

**10)  $A_{SEC}(1,1) = V_N(1,1,0) - m_1(1,1)$**  = amplitude of the secular light curve.  $A_{SEC}(1,1)$  is a measure of the activity of the nucleus. The value is calculated at (1,1) to allow comparison of different comets. Do not confuse with  $A_{ROT}$  the amplitude of the *rotational* light curve.

**11) D<sub>EFFE</sub>**, the effective diameter of the comet. It is common to see the effective diameter defined in the literature as  $D = (a \cdot b \cdot c)^{1/3}$ . However the mean nuclear magnitude of a nucleus of semi-axis a, b, c, is defined in terms of the *mean V value* of the *rotational* light curve, thus it is important to see to what diameter this magnitude corresponds to

$$V_{MAX} = C + 2.5 \text{ Log } a \cdot c \quad (6)$$

$$V_{MIN} = C + 2.5 \text{ Log } b \cdot c \quad (7)$$

$$V(1,1,0) = V_{NUC} = (V_{MAX} + V_{MIN})/2 = C + 2.5 \text{ Log } (a \cdot b \cdot c^2) \quad (8)$$

$$D_{EFFE} = 2 (a \cdot b \cdot c^2)^{1/4} \quad (8)$$

where C is the zero point constant and  $a \geq b \geq c$ . Notice the weight of semi-axis c which is usually poorly determined and thus assumed equal to b. Then

$$D_{EFFE} \sim 2 (a \cdot b^3)^{1/4} \quad (9)$$

These values of the effective diameter correspond to the middle of the rotational light curve. The diameter of the nucleus is customarily derived from the formula (Jewitt, 1991):

$$p_V r_N^2 = 2.24 \times 10^{22} R^2 \Delta^2 10^{0.4(m_\odot - m + \beta \alpha)} \quad (10)$$

where  $p_V$  is the geometric albedo,  $r_N$  is the nuclear radius,  $m_\odot$  is the solar magnitude ( $V_\odot = -26.74$ ,  $R_\odot$

= -27.10), m is the observed magnitude, R is the Sun-comet distance,  $\Delta$  is the Earth-comet distance,  $\alpha$  is the phase angle, and  $\beta$  the phase coefficient. In this equation r is given in meters, and R and  $\Delta$  are in AU.

Equation (10) can be simplified considerably if a) we use the absolute nuclear magnitude  $V_N(1,1,0)$ , b) if we replace the radius by the effective diameter,  $D_{EFFE}$ , and c) if we calculate this value in km not in m. The result is a much more compact and amicable formula:

$$\text{Log } [p_V D_{EFFE}^2 / 4] = 5.654 - 0.4 V_N(1,1,0) \quad (11)$$

if the absolute nuclear magnitude in the visual,  $V_N(1,1,0)$ , is used. If instead, the absolute nuclear magnitude in the red is used,  $R_N(1,1,0)$ , then:

$$\text{Log } [p_R \cdot D_{EFFE}^2 / 4] = 5.510 - 0.4 R_N(1,1,0) \quad (12)$$

Notice that now in these two formulas  $D_{EFFE}$  (in km),  $V_N(1,1,0)$ , and  $R_N(1,1,0)$  *all correspond to the mean value of the rotational light curve.*

**12) P-AGE** = Photometric Age. It is an objective of this work to be able to define a parameter that measures the age of a comet solely from the secular light curves. Although it is not possible in most cases to assign an absolute physical age (exception 2P/Encke), it is nevertheless possible to define a parameter related to

activity that ranks the comets by age. We call it P-AGE to distinguish it from a real age. It should be emphasized that P-AGE is not a dynamical age (although it may be related to it), but rather it is related to the loss of volatiles as a proxy for age. The ability to order comets according to their relative ages could be a useful tool to understand a number of events in the history of these objects.

Consider the three parameters  $A_{SEC}$ ,  $R_{ON}$  and  $R_{ON}+R_{OFF}$ . As a comet ages, the amplitude of the secular light curve,  $A_{SEC}$ , must decrease. In fact  $A_{SEC}$  must be zero for an inert nucleus. Thus  $A_{SEC}$  must be related to activity and age. *In this work we take both as synonymous. In fact activity is a proxy for age.*  $R_{ON}$  is also related to age. As the comet ages, the crust on the nucleus increases in depth, sublimating ices must recede inside the nucleus, sustained sublimation is quenched, and the comet needs to get nearer to the sun to be activated (Yabushita and Wada, 1988; Meech, 2000). Thus  $R_{ON}$  decreases with age. On the other hand,  $R_{ON}+R_{OFF}$  measures the total space of activity of the comet. Comets that have exhausted their CO and CO<sub>2</sub>, must get nearer to the sun to be active. In fact, water ice comets get active much nearer to the sun than CO or CO<sub>2</sub> dominated comets (Delsemme, 1982; Meech, 2000). Thus a parameter that measures age and activity at the same time, and that includes the three above quantities could be  $A_{SEC} * (R_{ON} + R_{OFF})$ . This value defines the area of a rectangle in the phase space  $A_{SEC}$  vs  $R_{SUM}$ .

So defined, P-AGE would give small values for old comets and large values for new comets, inverted from what we would like. It would be interesting to scale these values to human ages. We will call these “*comet years*” to reflect the fact that they have not yet been scaled to Earth’s years. To calibrate the scale, we will arbitrarily set to 28P/Neujmin 1 an age of 100 cy. With this calibration we define P-AGE thus:

$$P-AGE = 1440 / [A_{SEC} * (-R_{ON} + R_{OFF})] \text{ comet years (cy)} \quad (13)$$

Scaling to human ages may seem naïve and unorthodox. However it places the comets in perspective and provides a scale to compare with. This enhances the usefulness of P-AGE, and when the evolution of  $A_{SEC}$ ,  $R_{ON}$  and  $R_{OFF}$  with time is studied and calibrated with a suitable physical model, it will be possible to convert these values to a real physical age, thus achieving the objective we have set in this paper. The validity of this parameter is tested in several circumstances but we can say in advance that it classifies the secular light curves by shape, an interesting property and a proof of its validity.

The definition of P-AGE is robust, meaning that even if there are large errors in the input parameters, P-AGE comes out with a small error. This is due to the mathematical definition (Equation 13).

Consider the following: a) Since the onset and offset of activity are very sudden affairs, the error in the determination of  $R_{ON}$  and  $R_{OFF}$  is very small. So is the

error of  $A_{SEC}$ . b) If the slope of the secular light curve at onset or offset is uncertain, then  $R_{ON}$  or  $R_{OFF}$  increases when  $A_{SEC}$  decreases (or vice versa), and the product is insensitive to the variation. c) If only  $R_{ON}$  or  $R_{OFF}$  can be determined, the other one can be estimated from the mean  $R_{OFF}/R_{ON}$  value of the other comets ( $1.44 \pm 0.29$ ). Or from the maximum value for the asymmetry parameter (2.1 for comet 1995 O1 Hale-Bopp) you can get a lower limit (an upper limit can be obtained from the last observation). In conclusion, the error of P-AGE is small (as can be ascertained from the values and errors listed in the plots), and the definition is very robust. The same argument can be applied to the definition of T-AGE, given in the next section.

**13)  $n_{ON}$** , the slope parameter of secular light curve near the turn on point.

**14)  $n_{qB}$** , the slope of the curve just before perihelion.

**15)  $n_{qA}$** , the slope of the curve just after perihelion.

**16)  $R_{BP}$**  = Solar distance of the brake point in AU.

**17)  $m_{BP}$**  = magnitude of the brake point.

**18)  $A_{ROT}(PTV)$**  = peak to valley amplitude of the *rotational* light curve. This information is needed because all nuclear observations should lie inside the rotational amplitude.

## 4.2 Time plots

The following parameters are listed in the time plots. See Figure 4 for a graphical explanation of these parameters.

**19) LAG**, the shift in maximum light measured from perihelion in days.

**20)  $T_{ON}$  [days]** = the time at which the nucleus turns on. The negative sign in this parameter indicates pre-perihelion quantities. It corresponds to  $R_{ON}$  but in the time domain.

**21)  $T_{OFF}$**  = the time after perihelion at which the nucleus turns off.

**22)  $-T_{OFF}/T_{ON}$** , an asymmetry parameter but in the time domain.

**23)  $T_{ACTIVE} = (-T_{ON} + T_{OFF})$** , in days. It is a measure of the total time that the comet is active.

**24) T-AGE**= time-age. It is possible to define an age from the time plot in the same way we did for P-AGE:

$$T-AGE = 90240 / [A_{SEC} * (-T_{ON} + T_{OFF})] \text{ comet years (cy)} \quad (14)$$

**25) Perihelia.** The perihelia that contributed to the SLC, in the format YYYYMMDD.

**26)  $P_{ORB}$** , the orbital period around the Sun, in years.

**27)  $T_{\text{PERI-NEXT}}$**  , the *approximated* date of the next apparition for planning purposes.

**28)  $N_{\text{OBS}}$**  , the total number of observations used in the secular light curve.

**29)  $m_{\text{MAX}}(1, \text{LAG})$**  = maximum reduced magnitude measured at the time LAG. This value should change with orbital and time evolution.

**30)  $S_{\text{ON}}$**  = The slope of the envelope at  $T_{\text{ON}}$ , for planning purposes.

**31)  $S_{\text{OFF}}$**  = The slope of the envelope at  $T_{\text{OFF}}$ , for planning purposes.

**32)  $\langle p_v \rangle$**  = the mean value of the geometric albedo in the visual.

**33)  $\langle \beta \rangle$**  = the mean value of the phase coefficient. A Table of phase coefficients was published in paper II, and an updated list is kept at the web site cited at the end of this paper.

**34)  $\langle V-R \rangle$**  = the mean value of the color index V-R. A Table of color indexes was published in paper II, and an updated list is kept at the web site cited at the end of this paper.

### 5. Age-Size Classification

It is useful to classify comets by age and size. An histogram of diameters (see Figure 5) shows that

most JF comets are less than 10 km in diameter. Thus it is possible to define size classes thus:

- 0 < D < 1.5 km, dwarf comet, d.
- 1.5 < D < 3, small comet, s.
- 3 < D < 6 km, medium size comet, ms.
- 6 < D < 10 km, large comet, L.
- 10 < D < 50 km, giant comet, g.
- 50 < D , goliath comet, G

The same can be done for the age of a comet. Most comets have photometric ages less than 100 cy. Let us define:

- 0 < P-AGE < 4 cy, baby comet, b.
- 3 < P-AGE < 30 cy, young comet, y.
- 30 < P-AGE < 70 cy, middle age comet, ma.
- 70 < P-AGE < 100 cy, old comet, O.
- 100 cy < P-AGE, methuselah comet, M.

Using this classification we find that 1P/Halley is a young large comet (classified yL). We also find that comet 29P/SW 1 is a baby goliath comet (bG). 28P/Neujmin 1 and C/2001 OG108 LONEOS are methuselah giant comets (Mg). 107P/Wilson-Harrington and 133P/Elst-Pizarro are methuselah small comets (Ms). 67P/Churyumov-Gerasimenko and 85P/Boethin are middle age medium size comets (mams). And Sugano-Saigusa-Fujikawa turns out to be a middle age dwarf (mad).

Some researchers do not like to place comets into boxes and would argue that there is a continuum of ages and sizes. This is correct. Then an alternative scheme of classification is to give the two numbers P-AGE /  $D_{\text{EFFE}}$  taking into consideration that 90% of comets lie inside  $0 < \text{P-AGE} < 100$  cy and 95% inside  $0 < D_{\text{EFFE}} < 10$  km. *Any object above 100/10 or near 0/0 is exceptional.* For example 29P/SW1 with 0.7/54, *is exceptional.* In this scheme 1P/Halley has measurements 7/10, 28P/Neujmin 1 has 100/23, C/2001 OG108 has 102/16. Comets 107P/WH and 133P/E-P have respectively 1370/3 and 1640/5, while 85P/Boethin and SSF have 49/6 and 53/0.7.

A comparative diagram of the diameters of comets, can be found in Figure 6. It shows that there are a few very large comets that if they were to break they would give origin to thousands of minor comets.

## 6. Overview

Next we are going to describe several cometary phenomena deduced from the plots. It is beyond the scope of this Atlas to give a complete and coherent explanation of these phenomena. In a few cases we will only suggest some hypothesis. A statistical analysis of this data and a more in depth study of some of the physical phenomena will be carried out elsewhere.

### 6.1 General

- **Phases of the SLC.** It can be seen that most comets have three phases in their secular light curves: a nuclear

phase ( $R < R_{\text{ON}}$ ), a coma phase ( $R_{\text{ON}} < R < R_{\text{OFF}}$ ), and again a nuclear phase ( $R_{\text{OFF}} < R$ ) (in the time domain  $\Delta t < T_{\text{ON}}$ ,  $T_{\text{ON}} < \Delta t < T_{\text{OFF}}$ , and  $T_{\text{OFF}} < \Delta t$ ).

- **Shape of the SLC and P-AGE.** The secular light curves have been organized by increasing ID number to facilitate their access. However it is also interesting to order them by P-AGE. It is then possible to see that P-AGE orders the comets by shape of the SLC, a most interesting property. Young comets with tall and wide SLCs come first, while old comets with short and thin SLCs come last.

- **H<sub>2</sub>O, CO and CO<sub>2</sub> ice sublimation.** Before P-AGE  $\sim < 30$  cy, some comets exhibit a linear slope at turn on. This is an indication of CO or CO<sub>2</sub> ice sublimation, because the vapor pressure curve of those substances is linear. The existence of CO has been determined in a number of comets. After P-AGE  $\sim 30$  cy, comets exhibit a SLC that shows curvature. Curvature is a clear indication of water ice sublimation, because the water vapor pressure vs temperature shows strong curvature and the SLC is a reflection of this law. The shape after turn on is an indicator of composition.

- **Threshold coma magnitude.** In Paper I it was shown that comet 28P/Neujmin 1 exhibited a coma with a secular amplitude  $A_{\text{SEC}}(1,1) = 3.2$  mag, while 133P does not exhibit a coma with  $A_{\text{SEC}}(1,R) = 2.3$  mag and 2P does not exhibit a coma at aphelion with  $A_{\text{SEC}}(1,R) = 2.7$  mag. Thus it seems that there is an intermediate value at

which the coma becomes undetectable. We call that a threshold coma magnitude, TCM, and we estimate its value at  $TCM = \sim 3.0 \pm 0.3$  mag *above the nucleus*. Below TCM the *comet is active but the coma is below detection level* and the nucleus looks stellar.

- **Maximum value of  $A_{SEC}$ .** There seems to be a maximum value of the amplitude of the secular light curve,  $A_{SEC}(MAX) \sim 11.0 \pm 0.5$  mag. This number measures the maximum sublimating through output that a comet surface made of water ice can output.

## 6.2 Classes of comets

Looking at the plots new classes of comets arise:

**1) Comets with power laws at turn on.** Several comets exhibit power laws at turn on. This is an indication that they are sublimating something more volatile than water ice, because water ice shows curvature. Comets that belong to this class are listed in Table 1. It can be seen that all are young comets.

Notice that only 6 comets out of 26 (23%) exhibit power laws at turn on, and the ones that do so, do so only partially. Table 1 gives evidence to conclude that the predictive power of the H10 system is restricted to young comets with power laws.

**2) Comets with power law brake.** Young comets have a tendency to exhibit a brake in the incoming branch of the SLC, where the curve changes slope abruptly. This

has been interpreted as a change from sublimating something more volatile than water ice (probably CO), to sublimating water ice. Comets that belong to this class are listed in Table 2. Once again we see that all comets in this category are young.

In most comets one single substance, water ice or CO<sub>2</sub> controls sublimation. If the interpretation of the brake is a change of controlling substance, then all comets with power law brakes are controlled by two substances. The best example of this is comet 9P. At turn on sublimation takes place causing a linear law, until at  $R = -2.08$  AU water ice takes over and curvature is then apparent.

**3) Comets with belly.** Young comets are also the only ones that exhibit a belly: 1P (P-AGE = 7 cy), C/1995 O1 HB (1.8 cy), 19P (14 cy), 9P (21 cy), 21P, (20 cy), 6P (24 cy).

**4) Comets with steep ascend at turn on.** Some comets exhibit a significant slope at turn on. Example, 6P with P-AGE = 24 cy has a slope at turn on of  $-0.17$  mag/d (in the log plot,  $R^{+70}$ ).

**5) Comets with steep descend at turn off.** Several comets exhibit a steep descent at turn off. Members of this class are 1P, 85P, C/1996 B2.

**6) Comets that turn on after perihelion.** Two methuselah comets exhibit activity only past perihelion (107P, 133P).

**7) Comets with outbursts after turn off.** 1P/Halley had a large outbursts *after turn off*, with  $\Delta m = -6.5$  magnitudes ( - sign indicates brighter, + sign fainter). This new class is opened because there is evidence to believe that comets 10P/Tempel 2 and comet 53P/van Briesboeck may also have exhibited this kind of behavior in the past.

**8) Comets with activity at aphelion.** The only comet that belongs to this class is comet 2P/Encke. The amplitude of the activity is  $\Delta m = -2.7$  mag. Aphelion activity is suspected in comet 133P/Elst-Pizarro.

**9) Comets with an "S"-shaped SLC.** Two comets exhibit an S-shape of the SLC (19P and C/2001 OG108), both after perihelion. There is no current explanation for this feature.

**10) Comets with Extreme LAG.** Several comets exhibit extreme value of LAG. The most likely explanation is that the pole of the nucleus lies near the orbital plane and the pole points to the Sun at time = LAG. Members of this class, 6P (LAG= +46 d), 65P (+242 d), 107P (+42 d), 133P (+155 d), and C/1995 O1 (+45 d). 101P is the only one with a significant *negative* LAG, LAG= -126 d. Positive LAGs are more common than negative LAGs (13 vs 6).

**11) Spill over comets.** Definition: "*A spill over comet is one that does not reach to its nuclear magnitude when it reaches to aphelion*". Thus the object spills over its activity from one orbit to the next. Members of this class

are 29P, 39P, 65P, 73P/SW3C in 1990, 81P. Probable members are 9P and 19P.

**12) Comets with q-effect.** Definition: "*The q-effect or perihelion effect is a change in the maximum brightness exhibited by a comet at perihelion, as a consequence of a change in perihelion distance*". Several comets exhibit this effect, one of the most significant being 101P/Chernykh which shows a change of perihelion distance of -0.212 AU causing a change of -4.9 mag/AU.

**13) Comets with photometric anomalies.** Several comets exhibit a photometric anomaly :

- **1P/Halley.** Exhibits a small photometric anomaly post-perihelion, of  $\Delta m = +0.5$  mag amplitude. The confirmation that this is a real feature is that the same deep appears at the same place in infrared  $J_0$  and visual  $C_2$  observations (Morris and Hanner, 1993).

- **2P/Encke** exhibits a deep in the SLC *at aphelion*, of  $\Delta m = +1.7$  mag. The magnitude decays linearly until it reaches the nucleus (confirmation the plot in Additional Plots).

- **67P/Churyumov-Gerasimenko** exhibits a decrease in brightness just before perihelion of  $\Delta m = +1.9$  mag. This could be the result of a topographic effect. Alternatively this feature could be interpreted as a "S-shape" like the ones exhibited by comets 19P and C/2001 OG108 *before* perihelion.

- **Comet C/1995 O1 Hale-Bopp** exhibits an increase in brightness *above the power law*, centered at perihelion of  $\Delta m = -3.4$  mag. This is a *perihelion surge* since it is symmetric with respect to  $q$ .

- **Comet C/1996 B2 Hyakutake** shows a most peculiar increase in brightness at minimum approach to Earth, of  $\Delta m = -1.1$  mag. We would expect a decrease in brightness due to the Delta-effect (Kamel, 1997). However what is observed is *an increase* in brightness. The explanation of this discrepancy is that comet C/1996 B2 had many outbursts along the orbit (Schleicher and Osip, 2002) and by chance one of them took place near  $R = 1$  AU, masking any Delta-effect.

While the photometric anomalies of 1P, 2P and 67P might due to a topographic feature, the perihelion surge of Hale-Bopp might be due to boiling sublimation at perihelion, or sublimation of a substance much more volatile than H<sub>2</sub>O.

### 6.3 Odd comets.

Definition of a normal comet: *A normal comet is one that exhibits sustained activity quasi-symmetric with respect to perihelion, within a well defined turn on point before perihelion, and a well defined turn off point after perihelion.* Based on this definition, some comets listed below, are not normal.

**6P/D'Arrest.** Has a very asymmetric light curve with LAG = +48 d. It is difficult to measure its absolute magnitude. *The nucleus has a very odd shape, or the distribution of volatiles on the surface is very odd, or both.*

**9P/Tempel 1.** While the sublimation of most comets is controlled by one substance, the sublimation of 9P is controlled by two substances. In the log plot it can be seen how at turn on the slope is linear (clear indication of CO sublimation) and at  $R = -2.08$  AU it converts to a law with curvature (clear indication of H<sub>2</sub>O sublimation).

**19P/Borrelly.** Shows an odd shape of the SLC after perihelion in the form of an "S". At the present time there is no explanation for this feature.

**29P/SW 1.** This comet is permanently beyond Jupiter. It does not exhibit a regular SLC. It shows an irregular activity reminiscent of "boiling". It is active all around the orbit at 5.9 AU from the Sun.

**67P/Churyumov-Gerasimenko.** The photometric anomaly pre-perihelion of this comet is very intense and unique.

**101P/Chernykh.** The SLC is asymmetric exhibiting a huge pre-perihelion LAG. *The nucleus has a very odd shape, or the distribution of volatiles is very odd, or both.*

**107P/Wilson-Harrington.** The activity was detected photographically in only one night in 1949. This is one of

the oldest comet measured by P-AGE of this Atlas, and the SLC is like no other.

**133P/Elst-Pizarro.** This methuselah comet besides presenting a brief activity after perihelion, exhibits a very thin tail that does not widen with distance. This is at odds with normal tails that widen.

**C/2001 OG108.** Shows an odd shape of the SLC after perihelion in the form of an "S". At the present time there is no explanation for this feature.

#### 6.4 Look alike comets

Although there are not two comets that are identical, some have look alike SLCs. For example compare the ones in Table 3. In most cases the pair has about the same P-AGE, but not always.

### 7. Comments on specific comets

#### Log Plots

**1P/Halley, Log plot.** Since this young large comet has  $q < 1$  AU,  $\text{Log } 0.587 = 0.231$  has been subtracted before perihelion and added after perihelion to the horizontal axis to make room for observations inside the Earth's orbit. We can observe the three phases of the secular light curve, the nuclear phase, the coma phase and the nuclear phase again. On log plots power laws plot as straight lines, therefore the nucleus makes a pyramidal line at the bottom, since it follows a  $R^{+2}$  law. Most nuclear magnitudes lie inside the amplitude of the

*rotational* light curve range ( $A_{\text{ROT}}$ ). The turn-on and turn-off points are very sudden affairs, so it is easy to decide what is a nuclear magnitude and what observations are coma contaminated. The coma is described by two power laws before and one after perihelion. There is a noteworthy brake in the slope at  $R = -1.70$  AU for no apparent reason although we suspect it is due to the onset of water sublimation. The coma reaches a pointed sharp maximum after perihelion, and turns off with a steep descent. There is an outburst of 6.7 mags after the nucleus turns off. The secular light curve is very asymmetric with  $R_{\text{OFF}} / R_{\text{ON}} = 2.02$ . SEK = Sekanina (1985).  $V1+V2+G =$  Keller et al., (1987), based on Vega 1, Vega 2 and Giotto observations. CF (Campins and Fernandez, 2002).

**2P/Encke, log plot, 2003.** The x-axis has been increased in  $\text{Log } q = \pm 0.47965$  to make room for observations inside the Earth's orbit of this old medium size comet. The slope 5 line at the bottom of the plot in the form of a pyramid is due to the atmosphereless nucleus. Notice the sharp turn on point, and the activity at aphelion evidenced by observations well above the nuclear line. Although the SLC exhibits almost the same turn on and turn off distances, the SLC is asymmetric at 1 AU from the Sun, as evidenced by the fact that the absolute magnitude before perihelion,  $m_{1B}(1,1) = 9.8 \pm 0.1$ , while after perihelion is  $m_{1A}(1,1) = 11.5 \pm 0.1$ , an asymmetry of  $1.7 \pm 0.15$  magnitudes at 1 AU. The photometric age derived from this plot is  $P\text{-AGE} = 97 \pm 8$  cy (comet years), corresponding to an old comet. The mean value  $\langle V-R \rangle$  and  $p_R$  are taken from the literature. The

vertical distribution of nuclear observations are from Fernandez et al. (2005). The nuclear line is defined from paper IV.

**2P/Encke, log plot, 1858.** The SLC from 1858 compared with the SLC from 2003. The data has been taken from Kamel (1992). The SLC has been narrowing with time, a result that is in accord with the time evolution of the comets presented in this Atlas. It is possible to derive a photometric age for this Epoch. Seven physical parameters show evolution with respect to 2003.

**6P/D'Arrest Log plot.** The SLC of this young dwarf comet is very odd. Because the comet has a very large LAG= +46 d (confirmation the time plot), the log plot is distorted. It is then very difficult to determine the absolute magnitude. We know from the log plot that  $A_{SEC} > 10.0$  mag. Since the maximum observed for comets in this Atlas is  $A_{SEC} \sim 11$ , then it is a good guess that  $A_{SEC}$  for 6P  $\sim 10$  to  $\sim 11$ . This makes the comet very active, and this is an indication of youth. The estimated values are P-AGE < 28 cy and T-AGE < 26 cy. Because the SLC exhibits a large LAG and a sudden turn on with a very steep power law, this comet must be very odd, either with an *odd shape or with an odd distribution of volatiles*, and a pole laying near the orbital plane. It is very probable that one pole points to the sun at LAG causing the maximum brightness. The nuclear line is defined using the pre-turn on observations.

**9P/Tempel 1, log plot.** This young medium size comet has a most peculiar light curve with a brake in the power

law at turn on. The slope changes abruptly at  $R = -2.08$ , and then exhibits curvature, clear indication of water ice sublimation. The comet presents activity pre-turn on that has to be studied more carefully. The post-perihelion branch is also anomalous because it exhibits a linear decay over the whole range. CJ = Chen and Jewitt (1994), FMLAPB = Fernandez et al. (2003), LTAWW = Lamy et al. (2001), LFC = Lowry et al. (2003), M et al. = Meech et al. (2000), S = Scotti (1995), LF= Lowry and Fitzsimmons (2001).

**19P/Borrelly, log plot.** Only one power law is needed to describe the envelope before perihelion of this young medium size comet. After perihelion the secular light curve shows an S-shape characterized by an upturn at perihelion, shown also by comet C/2001 =G108 LONEOS. The reason for this odd shape is unknown. The turn-off point is uncertain. The nuclear magnitudes are reasonably well determined and observations lie inside the rotational light curve amplitude. LTW = Lamy et al. (1998), BHSBOH = Buratti et al. (2003), MS = Mueller and Samarasinha (2002).

**21P/Giacobinni-Zinner, log plot.** Three power laws are needed to describe the light curve of this young medium size comet. Notice the sharp change in slope at  $R = -1.58$  AU. M = Mueller (1992), CJ = Chen and Jewitt (1994), H = Hergenrother (Scotti, 2001).

**26P/Grigg-Skejellerup, log plot.** The size and P-AGE of this comet indicates that it is a old small nucleus, and that can be confirmed from the fact that the secular light

curve is dominated by the nuclear phase, while the coma phase is of short duration. BRBS = Boehnhardt (1998), HL = Hergenrother and Larson (Scotti, 2001), LTLRH = Licandro et al. (2000), S = Scotti (1995).

**28P/Neujmin 1, log plot.** The nuclear phase of this methuselah giant comet dominates the light curve. This is a text book example of how the nucleus follows a  $R^{-2}$  law and the nuclear observations lie inside the *rotational* light curve amplitude. Notice for example the two clusters of vertical points post-perihelion. The comet is active for about 9 months, and the amplitude  $A_{SEC}$  of the secular light curve has diminished significantly in comparison with 1P/Halley. This is a Saturn family comet, as deduced from the fact that the aphelion distance  $Q = 12.07$  AU, is beyond Saturn, and that the orbital inclination is  $i = 14^\circ$ , indicating that it is neither a nearly isotropic comet nor a Jupiter family comet in the classification of Levison (1999). In the 2002 apparition the comet was in conjunction to the Sun at perihelion and the coma phase could not be observed. Campins et al. (1995) have recalculated the diameter and albedo of this comet changing the parameters assumed for the standard thermal model, and the resulting albedo is twice the former value (Campins et al., 1987). However notice that the diameters quoted in their Table 2 correspond to a sphere of the same projected area  $A^*$  at the maximum of the rotational light curve  $A^*$ , thus they are not effective diameters as defined in equations (12) and (13). The Epoch is 1913, which means a) that the coma photometry is poor, and b) that there is an urgent need for observations of the coma phase of this comet to test for

evolution. Thus the next opportunity will be in the next perihelion passage, in 2021.2, with observations starting around 2020.6. DMHD = Delahodde et al. (2001), JM = Jewitt and Meech (1988), CAM = Campins et al. (1987).

**29P/Schwassmann-Wachmann 1, log plot.** This baby goliath comet exhibits an irregular light curve and must be classified as odd. There is no clear trend with solar distance. The comet is in a state of "boiling" with irregular outburst spaced along the orbit. The extrapolation of these magnitudes to perihelion result in the determination of a photometric age  $P-AGE = 0.7 \pm 0.2$  cy, clearly a baby comet. The nucleus dimensions are due to Stansberry et al. (2004).

**32P/Comas-Sola, log plot.** This middle age small comet has a well defined SLC. The apparitions of 1927-1969 require a correction of +0.82 mag, while that of 1978 requires +0.31 mag to place them at the level of 1996. Thus this comet has been decreasing significantly in brightness. The nuclear line is due to Tancredi et al. (2006).

**39P/Oterma, log plot.** This young medium size comet has a  $q = 3.39$  AU and thus never gets near to the sun. Its activity is restricted from  $q$  to  $Q$  and it is active all around the orbit. There is no nuclear phase. The comet has recently suffered an encounter with Jupiter that changed the orbit. The new  $q = 5.47$  AU and the new  $Q = 9.01$  AU. Thus the comet went from being a JF comet to a Centaur. Consequently the activity will be reduced further and it is expected that it will only raise  $\sim 3$

magnitudes above the nucleus. This value is identical to the threshold coma magnitude defined above, and thus it is probable that the comet will not exhibit a coma in this new orbit. This is an annual comet that can be observed all around the orbit. The comet resembles 65P/Gunn. It has not been ascertained if this comet is in the sustained regime or in the outburst regime. The nuclear magnitude is that deduced from Fernandez's observations in IAUC7689.

**45P/Honda-Mrkos-Pajdusakova, log plot.** The light curve of this middle age dwarf comet of only 0.9 km diameter is well defined, and allows the determination of numerous physical parameters, listed inside the plot. Notice the asymmetry of the SLC, and the steep descent at turn off, which marks the initiation of the nuclear phase. Although the comet exhibits a belly, actually it is not, and this is due to the fact that the comet has a very small perihelion distance of  $q = 0.53$  AU and often the behavior inside the Earth's orbit is a linear increase or decrease. This comet has some resemblance to C/1983 J1 Sugano-Saigusa-Fujikawa. LTAW = Lamy et al. (1999).

**65P/Gunn, log plot.** This young medium size comet resembles 39P/Oterma. In fact both had orbits inside Jupiter's orbit, before 39P was moved to an external orbit. 65P/Gunn does not have a nuclear phase being active all around the orbit. This is an annual comet. Notice the asymmetry before-after perihelion caused by a strong perihelion LAG observed in the time plot. The most probable explanation is that the pole of this comet lies

near the orbital plane and that it points to the Sun at time = LAG. The nuclear magnitude is due to Tancredi et al. (2006).

**67P/Churyumov-Gerasimenko, log plot.** By this P-AGE the secular light curve of this middle age medium size comet adopts a rounded shape that can not be described by a power law. Notice the existence of a photometric anomaly in the secular light curve from  $\text{Log } R = -0.27$  to  $\text{Log } R = -0.12$ . This piece of the secular light curve is enlarged and flattened in additional plots. This comet will be visited in 2014 by the spacecraft Rosetta. The location of the encounter, orbiter, landing and  $R_{ON}$  have been indicated. HM = Hainaut and Martinez (2004), LTWJK = Lamy et al. (2003), M = Mueller (1992), TFRL = Tancredi et al. (2000).

**73P/Scwassmann-Wachmann 3C, log plot, 1990 and 1995.** This is a splitted middle age small comet for which the SLC from 1990 and 1995 are quite different. Notice the huge increase in brightness in 1995. Consequently the photometric age also changed. In 1990 we find P-AGE = 55 cy while in 1995 we find 21 cy. The comet rejuvenated due to the outburst. This comet teaches us that a splitting *produces* an outburst. However small outburst may be due to surface activity and not to an splitting. The nucleus observations are from Boehnhardt et al. (1998).

**73P/Scwassmann-Wachmann 3C, log plot, 2001.** The SLC in 2001 still contained a lot of activity and the photometric age is comparable to that of 1995, P-AGE =

18 cy. Notice that the activity seems to reach to aphelion both pre and post perihelion.

**81P/Wild 2, log plot.** Different symbols correspond to different apparitions identified in the time plot. This young medium size comet exhibits a photometric behavior requiring three power laws, as for comet 1P/Halley. Notice the change in slope at  $R = -1.88$  AU. Pittichova and Meech (2001) found the comet active at  $R=4.98$  AU post-perihelion ( $\text{Log } R=0.70$ ), while aphelion takes place at  $R=5.3$  AU ( $\text{Log } R=0.72$ ). Thus it is likely that this comet is active at aphelion. It is even plausible that this comet may be active *beyond* aphelion, in which case it would be a member of the *spill-over comets*, comets whose activity spills over from one orbit to the next. Comets 19P and 21P might belong to this class too. The 2003 perihelion could not be observed because the comet was in conjunction with the Sun. Notice the secular increase in brightness with time: The 1990 observations had to be raised by 1.25 mag, and the 2003 apparition seems to have had a brighter maximum magnitude. LTLRH = Licandro et al. (2000), CJ = Chen and Jewitt (1994), LFC = Lowry et al. (2003), SEK = Sekanina (2003), MN = Meech and Newburn (1998), B et al. = Brownlee et al. (2004).

**85P/Boethin, log plot.** This middle age medium size comet has been selected as the next target of the extended Deep Impact Mission. It is a middle age comet with  $P\text{-AGE} = 49$  cy. Notice the large slope at turn on, with  $n = 28$ . The comet changed orbits from 1975 to 1986. Although  $q$  was larger in 1986, the comet was

brighter which does not make much sense. The nuclear magnitude of this comet can be derived from the two post perihelion observations of Roemer listed by Kamel (1992).

**101P/Chernykh, log plot.** This young medium size comet belongs to the class of odd comets. It exhibits a very strong LAG before perihelion. The plot had to be folded at  $q$ , because the folding at  $R = 1$  AU did not make much sense. Notice also that the observations in 1992 with smaller  $q$  are brighter than the 1978 observations, as expected. This comet splitted in 1991 April 15 at  $R = -3.32$  AU, thus this SLC must be anomalous. The nuclear lines are due to Scotti (1995) and Tancredi et al. (2006).

**107P/Wilson-Harrington, log plot.** This methuselah small comet exhibited very feeble activity in 1949 so there is the question if this is a comet or not. If a solar system object exhibits a tail, it must be a comet. Applying this definition to 107P, and considering other physical properties, it is concluded that this is a comet, albeit a rather old one. The calculation of the photometric age gives a very large value of  $P\text{-AGE} = 1370$  cy, a methuselah nucleus. The nuclear magnitude is derived from data compiled in this work.

**109P/Swift-Tuttle, log plot.** This middle age giant comet has a very pointed light curve with a very large slope at  $R = 1$  AU. Notice the smoothness of the envelope pre-perihelion. The nucleus line is due to Ó'Ceallaigh et al. (1995).

**133P/Elst-Pizarro, Log plot.** Most of the data is taken after perihelion, where this methuselah medium size comet shows a brief outburst. In order to calculate the photometric age of the comet, the amplitude of the secular light curve at  $R=1$  AU must be known,  $A_{SEC}(1,1)$ . Due to the lack of a suitable physical model for this type of object, we have chosen to use the light curves of 4 other comets as *templates* for extrapolation. In this way the estimated magnitude at  $R=1$  AU is  $10.0 \pm 1.6$  magnitudes, and the amplitude of the secular light curve is then  $A_{SEC}(1,1) = 6.0 \pm 1.5$ . In this way a P-AGE = 1460 cy can be calculated. However a calculation using time-Age giving a value of T-AGE = 80 cy. The Asteroid Dynamic Site data is plotted as open squares, and is used to corroborate the photometric data (black circles and squares). The magnitude increase at  $\text{Log } R = +0.516$  has not been corroborated with independent measurements. The main outburst is not well sampled. Two magnitudes near aphelion and 0.6 magnitudes above the nucleus, may suggest activity at aphelion. The turn off is determined with great accuracy thanks to our own observations (downward open triangles) and to serendipitous observations made by Lowry and Fitzsimmons (2004)=L&F (dark up triangles), HJF= Hsieh et al. (2004). The nuclear magnitude is by Hsieh, Jewitt and Fernandez (2004) = HJF.

**C/1983 H1 IRAS-Araki-Alcock, log plot.** This old medium size comet approached Earth within a very small distance. The SLC allows the determination of P-AGE = 76 cy, an old comet. The nuclear line is due to Sekanina (1988).

**C/1983 J1 Sugano-Saigusa-Fujikawa, log plot.** Since observations of this middle age dwarf comet were carried out only after perihelion, we had to assume a light curve before perihelion. It is clear from looking at other SLCs, that comets past middle age have almost symmetrical light curves. Thus we find P-AGE = 53 cy, a middle age comet. Unfortunately due to the eccentricity being  $e=1$ , the comet will not return in the near future. Notice that this is a very small comet of diameter  $D=0.7$  km. This value and the nuclear line come from Hanner et al. (1987).

**C/1985 XII Shoemaker, log plot.** The nucleus of this comet has not been observed, so we only have an upper limit. The turn off point can be determined with some precision, but the turn on point is unknown. To determine P-AGE we follow an iteration. We first assume  $R_{ON} = R_{OFF}$  and calculate P-AGE with  $A_{SEC} = 9.6$ . We find that it has a very small P-AGE and that the SLC resembles that of comet C/1995 O1 Hale Bopp or that of comet 1P/Halley. It is then reasonable to assume that  $R_{OFF} / R_{ON} = 2.04$  similar to those two comets. Then  $R_{ON} = 11.8$  AU, and P-AGE can be iterated to a second more precise value of P-AGE  $\sim 4.3$  cy, corresponding to a young giant object. MHM = Meech, Hainaut, Marsden (2004).

**C/1995 O1 Hale-Bopp, log plot.** Notice the sharp turn on and turn off points of this baby giant (or perhaps goliath) comet. Compare this SLC with that of comet 1P/Halley. They look very similar. Notice the perihelion

surge at  $q$ . There is no consensus on the nucleus diameter of this comet, so we plotted the maximum and minimum values. Notice the brake point at  $R=-6.3$  AU pre-perihelion. The nucleus size and the nuclear line of this comet are quite uncertain. The maximum value is due to Fernandez et al. (1999), while the smaller value is due to Schleicher et al. (1997). RB = Rivkin and Binzel (IAUC 8479), TS= Tsumura (2006).

**C/1996 B2 Hyakutake, log plot.** This was a bright young medium size comet that approached Earth, but it can be seen that its greatness was more due to the approach than to its absolute magnitude of  $m(1,1)= 4.3$ . The approach was at  $\Delta= 0.10$  AU but the SLC does not exhibit any decrease or increase, thus no evidence of a Delta effect. What is apparent at minimum approach is an increase in brightness, a kind of inverse delta effect. This is most apparent in the time plot. The comet had an outburst at this time masking any delta effect (Schleicher and Osip, 2002). The nuclear line is due to Lisse et al. (1999).

**C/2001 OG108 LONEOS, log plot.** This methuselah goliath comet exhibits an odd shaped light curve, with a prominent S-Shape that up to now does not have a physical explanation. It is a methuselah comet with  $P-AGE= 102$  cy. Although far into the future the comet will return in 2050. This is a large comet with  $D= 15.8$  km. The nuclear line is due to Abell et al. (2005).

## Time Plots

**1P/Halley, time plot.** This secular light curve is unusual in that the comet exhibits a prominent belly, in fact looking as a pregnant comet. The turn-off of activity is a very sudden event. Additionally the nucleus had a significant outburst at  $\Delta t = + 1772$  d. The thermal wave penetration into the nucleus, is clearly seen, thus sublimation must be taking place *in depth*.

**2P/Encke, time plot, Source 1, 2003.** Notice the time delay between maximum brightness and perihelion, LAG. The time-age derived from this plot is  $T-AGE= 103\pm 9$  cy, corresponding to a methuselah comet.

**2P/Encke, time plot, Source 1, 1858.** This figure confirms the findings of the log plot. There is a significant difference between the two apparitions. The shift of the SLC from 1858 to 2003 is what is expected from cometary evolution: a narrowing of the SLC and a decrease in absolute magnitude. Since this conclusion is derived from a SLC all past criticisms about fading of comets not been realistic, do not apply to this case. Other comets in this Atlas exhibit a narrowing of the SLC with  $P-AGE$ .

**6P/D'Arrest, time plot.** This comet has one of the largest values of  $LAG = +46$  d. This causes a distortion of the SLC making difficult the determination of some parameters. The turn on point exhibits a very large slope of  $0.17$  mag/d. The turn off is indeterminate.

**9P/Tempel 1, time plot.** Notice the rounded shape of the secular light curve, and possible activity before turn on.

**19P/Borrelly, time Plot.** The secular light curve exhibits a prominent belly after perihelion. The turn-off is beyond 320 days.

**21P/Giacobinni-Zinner, time plot.** The brake in the SLC can be detected in this plot before perihelion. The turn off is not well determined.

**26P/Grigg-Skejellerup, time plot.** Notice the round shape of the secular light curve characteristic of old comets and water ice sublimation, and the short time of activity that does not reach 7 months.

**28P/Neujmin 1, time plot.** Notice the round shape of the secular light curve and the short interval of activity. The Epoch of this plot is 1913 which implies that the photometry must be poor and that there is an urgent need to observed this comet in the coma phase. In 2003 perihelion coincided with conjunction with the Sun, so the coma phase went unobserved. The next opportunity will be in October of 2020.

**29P/Schwassmann-Wachmann 1, time plot.** The SLC shows that the comet is active all around the orbit. So observers should look for periods of inactivity to observe the nucleus. These are infrequent.

**39P/Oterma, time plot.** This comet is active all around the orbit. The comet is annual. The turn on and turn off points are beyond aphelion. LAG= 0 for this comet.

**45P/Honda-Mrkos-Pajdusakova, time plot.** The light curve is well defined. Notice the steep descent at turn off. The comet practically has no lag. Notice that this is a dwarf comet of only 0.9 km diameter. Although the comet exhibits a belly, actually it is not, and this is due to the fact that the comet has a very small perihelion distance of  $q = 0.53$  AU and often the behavior inside the Earth's orbit is a linear increase or decrease. This comet has some resemblance to C/1983 J1 Sugano-Saigusa-Fujikawa.

**65P/Gunn, time plot.** This comet is very similar to 39P but with a perihelion LAG= +242 d, a huge value. A probable interpretation is that the nucleus' pole points to the sun at LAG.

**67P/Churyumov-Gerasimenko, time plot.** Notice the rounded shape of the secular light curve and the uncertainty in the nucleus magnitude. The photometric anomaly has been expanded in an additional plot.

**73P/Schwassmann-Wachmann 3C, 1990 and 1995, time plot.** This comet experienced an outburst, changing the SLC from 1990 to 1995. Due to the outburst the comet *rejuvenated*, its P-AGE going from 55 cy in 1990 to 21 cy in 1995. There is no way to calculate a T-AGE because we do not know the turn off date. This plot shows that every splitting is accompanied by an outburst.

And we are also allowed to conclude that no outburst, no splitting. The two outbursts had about the same amplitude, 6.4 vs 6.3 magnitudes.

**73P/Schwassmann-Wachmann 3C, 2001, time plot.** The comet seems to be even more rejuvenated.

**81P/Wild 2, time plot.** Notice the secular increase in maximum brightness.

**85P/Boethin, time plot.** This middle age comet exhibits a round SLC typical of water ice dominated comets.  $R =$  Roemer.

**107P/Wilson-Harrington, time plot.** The activity of this comet took place is a few nights, thus it is not surprising that its T-AGE is 720 cy, a methuselah comet.

**109P/Swift-Tuttle, time plot.** This young giant comet has a very smooth light curve. Unfortunately this comet will not be seen for another century.

**133P/Elst-Pizarro, time plot.** The shape of the outburst is clearly seen, as well as the possible activity at aphelion. The outburst was initiated at  $T_{ON} = 42 \pm 4$  d (Sekanina, IAUC 6473), reached a maximum amplitude of  $A_{SEC}(1,R) = 2.3 \pm 0.2$  magnitudes at  $LAG = 155 \pm 10$  d, and turned off at  $T_{OFF} = 233 \pm 10$  d. A Time-Age, T-AGE = 80 (+30, -20) cy can be calculated from this plot. We believe this value is more related to reality, by comparison with comet 26P which 133 resembles. By good luck our own observations (open down triangles)

and those of Lowry and Fitzsimmons help define the extent of activity. The date of the next perihelion is indicated. L&F= Lowry and Fitzsimmons (2005).

**C/1983 H1 IRAS-Araki-Alcock, time plot.** This famous comet approached Earth at very short distance. The SLC is somewhat uncertain, but there is evidence that this comet is old.

**C/1983 J1 Sugano-Saigusa-Fujikawa, time plot.** The SLC of this comet is somewhat uncertain, but there is evidence to conclude that this is an old comet.

**C/1995 O1 Hale-Bopp, time plot.** Compare this plot with that of comet 1P/Halley. They are very similar, both with an extensive belly. Notice that the surge is not apparent in the time plot. RB = Rivkin and Binzel (IAUC 8479), TS= Tsumura (2006).

**C/1996B2 Hyakutake, time plot.** The comet exhibits a normal SLC with a very small negative LAG. There is a photometric anomaly at  $t \sim -39$  d, seen expanded in a view in additional plots due to a water outburst (Schleicher and Osip, 2002).

**C/2001 OG 108 LONEOS, time plot.** This very old Halley type comet exhibits the same S-shaped anomaly as 19P/Borrelly. The origin of this feature is unknown. The reason for having observations well below the nucleus is not understood either.

## Additional Plots

**1P/Halley, photometric anomaly.** The brake point is clearly seen. The brightness changes slope abruptly at perihelion. The gaps at perihelion and at  $\text{Log } R = +0.75$  are due to conjunction with the Sun. There is a deep in the SLC from  $R = +1.11$  AU to  $R = +1.24$  AU, of amplitude  $m = 0.5 \pm 0.1$  mag, or  $T = +45$  to  $+56$  d. The reason we believe this photometric anomaly is real is because there was a deep in the  $C_2$  production rate and the  $J_o$  infrared value, at  $R = +1.21$  AU (Morris and Hanner, 1993). Most probably this feature is due to a topographic effect.

**2P/Encke, time plot, photometric anomaly at aphelion, Source 2.** The dashed line tries to describe an envelope of the observations but in no way implies that the activity is sustained. Between  $\Delta t = +310$  and  $+392$  d there is a well observed linear decay in brightness that might be indication of topography. The maximum activity ( $2.7 \pm 0.2$  mag) is quite significant. The nuclear magnitude derived from the phase plot, is in agreement with the lowest observations at aphelion by Fernandez et al. (2005) and Meech et al. (2001) at  $\Delta t = +390$  days. The shape of the S2 light curve, is a reflection of that of S1.

**2P/Encke, photometric anomaly at aphelion, expanded.** The anomaly has been expanded from the previous Figure to see its extent and shape. The brightness decreases linearly from  $\Delta t = +310$  to  $+392$  d after perihelion, an interval of 82 days. There seems to be an absolute minimum of the secular light curve at  $\Delta t =$

$+393$  to  $413$ . The photometric anomaly can be due to a topographic effect or the turn off of an active region. Additional observations of this region are highly desirable because this might be the absolute minimum brightness of the whole orbit.

**67P/Churyumov-Gerasimenko, photometric anomaly.** This comet exhibits a prominent photometric anomaly from  $-119$  d to  $-6$  d before perihelion. It could be due to an odd shape of the nucleus, an odd distribution of volatiles, or to the turn off of an active region. The anomaly has an amplitude of 1.9 magnitudes, and observations from the apparitions of 1982, 1996 and 2002 show it, thus it must be a permanent feature of the SLC. The comet needs observations from November 3<sup>rd</sup>, 2008 to February 20<sup>th</sup>, 2009.

**C/1995 O1 Hale-Bopp, photometric anomaly.** This feature is placed exactly at perihelion, being approximately symmetric with respect to it. It is apparent an increase in brightness *above the power law*. This phenomena may be due to *boiling* of the surface or sublimation of a substance more volatile than water ice.

**C/1996 B2 Hyakutake, photometric anomaly.** The anomaly appears at the time of minimum approach, when we should expect the action of the Delta-effect. This effect is a decrease in brightness, but what is seen is *an increase* in brightness. A comparison with the water production rate shows that the brightness increase correlates with a water outburst.

Plots and tables in ASCII format can be downloaded from the site: <http://webdelprofesor.ula.ve/ciencias/ferrin>.

## **ACKNOWLEDGEMENTS**

Some secular light curves contain observations carried out at the National Observatory of Venezuela (ONV), managed by the Center for Research in Astronomy (CIDA), for the Ministry of Science and Technology (MinCyT). We thank the TAC of CIDA for assigning telescope time to observe these faint objects. To the Council for Scientific, Technologic and Humanistic Development of the University of the Andes for their support through grant number C-1281-04-05-B.

## REFERENCES

- Abell, P.A., Fernandez, Y.R., Pravec, P., Frech, L.M., Farnham, T.L., Gaffey, M.J., Handersen, P.S., Kusnirak, P., Sarounova, L., Sheppard, S.S., Narayan, G., 2005. Physical characteristics of comet nucleus C/2001 OG108 (LONEOS). *Icarus*, 179, 174-194.
- Belton, M.J.S., Wehinger, P., Wyckoff, S., Spinrad, H., 1986. A precise Spin Period for P/Halley , 599-603, in "20th Slab Symposium on the Exploration of Halley's Comet", Battrick, B., Rolfe, E.J., Reinhard, R., Editors, ESA SP-250, Vol. 1, Paris, France.
- Boehnhardt, H., Rainer, N., Birkle, K., Schwehn, G., 1998. The Nuclei of Comets 26P/Grigg-Skejellerup and 73P/Schwassmann-Wachmann 3, *Astron. Astrophys.*, 341, p. 912-917.
- Brownlee, D. E. And 11 colleagues, 2004. Surface of Young Jupiter Family Comet 81P/Wild 2: View from the Stardust Spacecraft. *Science*, 304, 1764-1769.
- Buratti, B.J., Hicks, M.D., Soderblom, L.A., Britt, D., Oberst, J., Hillier, J.K., (2003). Deep Space 1 Photometry of the Nucleus of Comet 9P/Borrelly. *Icarus*, 167, 16-29.
- Campins, H., A'Hearn, M.F., McFadden, L., 1987. The Bare Nucleus of Comet Neujmin 1. *Ap. J.*, 316, p. 847-857.
- Campins, H., Osip, D.J., Riecke, G.H., Rieke, M.J., 1995. Estimates of the radius and albedo of comet-asteroid transition object 4015 Wilson-Harrington based on infrared observations. *Planet. Space Sci.*, 43, 733-736.
- Campins, H., Fernandez, Y., 2002. Observational Constrains on the Surface Characteristics of Comet Nuclei. *EMP*, 89, p. 117-134.
- Chen, J., Jewitt, D., 1994, On the Rate at Which Comets Split, *Icarus*, 108, pp. 265-271.
- Delahodde, C.E., Meech, K.J., Hainaut, O.R., Dotto, E., 2001. Detailed Phase Function of Comet 28P/Neujmin 1, *Astron. Astrophys.*, 376, 621-640.
- Delsemme, A.H., 1982. Chemical Composition of the Cometary Nucleus, 85-130, in "Comets", L. Wilkening, Editor, Univ. Of Arizona Press, Tucson.
- Fernandez, Y.R., Wellnitz, D.D., Buie, M.W., Dunham, E.W., Millis, R.L., Nye, R.A., Stansberry, J.A., Wasserman, L.H., A'Hearn, M.F., Lisse, C.M., Golden, M.E., Person, M.J., Howell, R.R., Marcialis, R.L., Spitale, J.N., 1999. The Inner Coma and Nucleus of Comet Hale-Bopp: Results from a Stellar Occultation. *Icarus* 140, 205-220.
- Fernandez, Y.R., Meech, K.J., Lisse, C.M., A'Hearn, M.F., Pittichova, J., Belton, M.J.S., 2003, The Nucleus of Deep Impact Target Comet 9P/Tempel 1, 164, 481-491.
- Fernandez, Y.R., Lowry, S.C., Weissman, P.R., Mueller, B.A., Samarasinha, N.H., Belton, M.J.S., Meech, K.J., 2005. New Near-Aphelion Light Curves of Comet 2P/Encke. *Icarus*, 175, 194-214.
- Ferrín, I., 2005a. Secular Light Curve of Comet 28P/Neujmin 1, and of Comets Targets of Spacecraft, 1P/Halley, 9P/Tempel 1, 19P/Borrelly,

- 21P/Grigg-Skejellerup, 26P/Giacobinni-Zinner, 67P/Chryumov-Gersimenko, 81P/Wild 2. *Icarus* 178, 493-516.
- Ferrín, I., 2005b. Variable Aperture Correction Method in Cometary Photometry, *ICQ* 27, p. 249-255.
- Ferrín, I., 2006. Secular Light Curve of Comets: 133P/Elst-Pizarro. *Icarus*, 185, 523-543.
- Ferrín, I., 2007. Secular Light Curve of Comet 9P/Tempel 1. *Icarus*, 187, 326-331.
- Ferrín, I., 2008. Secular Light Curve of Comet 2P/Encke, a comet active at aphelion. *Icarus*, submitted for publication.
- Fink, U., Hicks, M. P., Fevig, R. A., 1999. Production Rates for the Stardust Mission Target: 81P/Wild 2. *Icarus*, 141, 331-340.
- Gehrels, T., 1999. A Review of Comet and Asteroid Statistics, *Earth Planets Space*, 51, 1155-1161.
- Green, D. W. E., 1991. Recent News and Research Concerning Comets. *ICQ*, 13, No. 79, 91-94.
- Green, D. W. E., 1997. *ICQ Guide to Observing Comets*. SAO, Cambridge, Mass., 100-103.
- Green, D., W. E., Editor, 2007. *Issues of the International Comet Quarterly*, SAO, Cambridge, Mass, USA.
- Hainaut, O., Martinez, M., 2004. ESO's Telescope Takes Picture of ESA's Rosetta Target, Comet 67P/Churyumov-Gerasimenko, ESO Press Photos 06<sup>a</sup>-b/04.
- Hanner, M. S., Newburn, R.L., Spinrad, H., Veeder, G.J., 1987. Comet Sugano-Saigusa-Fujikawa (1983 V) - A small puzzling comet. *An. J.*, 94, 1081-1087.
- Hicks, M.D., Bamberg, R.J., Lawrence, K.J., Kollipara, P., 2007. Near-Nucleus photometry of comets using archived NEAT data. *Icarus*, 188, 457-467.
- Hsieh, H. H., Jewitt, D., 2005. Search for Active Main - Belt Asteroids: The SAMBA Project. 37<sup>th</sup> DPS Meeting, Sept., Session 11, Abstract 11.01.
- Jewitt, D., Meech, K., 1988. Optical Properties of Cometary Nuclei and A Preliminary Comparison with Asteroids, *A.J.*, 328, p. 974-986.
- Jewitt, D. C., 1991. Cometary Photometry. In *Comets in the Post-Halley Era*. R. L. Newburn, M. Neugebauer, J. Rahe, Editors, Vol. 1, pp. 19-65, Kluwer, Dordrecht, Boston, London.
- Kamel, L., 1992. The comet light curve atlas. *Astron. and Astrophys.*, 92, 85-149.
- Kamel, L., 1997. The Delta Effect in the Light curves of 13 Periodic comets. *Icarus*, 128, 145-159.
- Keller, H.U. and 21 colleagues, 1987. Comet P/Halley's Nucleus and its activity, *Astron. Astrophys.*, 187, p. 807-823.
- Lamy, P. L., Toth, I., Weaver, H.A., 1998. Hubble space telescope observations of the nucleus and inner coma of comet 19P/1904Y2 (Borrelly). *Astron. Astrophys.*, 337, 945-954.
- Lamy, P., Toth, I., A'Hearn, M., Weaver, H.A., 1999. Hubble Space Telescope Observations of the Nucleus of Comet 45P/Honda-Mrkos-Pajdusakova and its Inner Coma", *Icarus*, 140, 424-438.
- Lamy, P.L., Toth, I., A'Hearn, M.F.A., Weaver, H.A., Weissman, P.R., 2001. Hubble Space Telescope Observations of comet 9P/Tempel 1, *Icarus*, 154, 337-344.
- Lamy, P.L., Toth, I., Weaver, H., Kaasalainen, M., 2003.

- The Nucleus of Comet 67P/Churyumov-Gerasimenko, the New Target of the Rosetta Mission, DPS 35th Meeting, September.
- Lamy, P.L., Toth, I., Fernandez, Y.R., Weaver, H.A., 2005. The Sizes, Shapes, Albedos and Colors of Cometary Nuclei. 317-335, In Comets II, Festou, M., Keller, H.U., Weaver, H. E., Editors, Univ. of Arizona Press, Tucson.
- Levison, H., 1999. Comet Taxonomy. In *Completing the Inventory of the Solar System*. T. Retting and J.M. Hahn, editors. ASP Conference Series 107. 173-191.
- Licandro, J., Tancredi, G., Lindgren, M., Rickman, H., Hutton, R.G., 2000. CCD Observations of Comet Nuclei, I: Observations from 1990-1995. *Icarus*, 147, pp. 161-179.
- Lisse, C.M., Fernandez, Y.R., Kundu, A., A'Hearn, M.F., Dayal, A., Deustch, L.K., Fazio, G.G., Jora, J.L., Hoffmann, W.F., 1999. The nucleus of comet Hyakutake (C/1996 B2). *Icarus*, 140, 189-204.
- Lowry, S.C., Fitzsimmons, A., Cartwright, L.M., Williams, I.P., 1999, CCD Photometry of Distant Comets, *Astron. Astrophys.* 349, 649-659.
- Lowry, S.C., Fitzsimmons, A., 2001. CCD Photometry of Distant Comets II. *Astron. and Astrophys.*, 365, 204-213.
- Lowry, S.C., Weissman, P.R., 2003. CCD Observations of Distant Comets From Palomar and Steward Observatories. *Icarus* 164, 492-503.
- Lowry, S.C., Weissman, P.R., Sykes, M.V., Reach, W.T., 2003. Observations of Periodic Comet 2P/Encke: Physical Properties of the Nucleus and First Visual-Wavelength Detection of Its Dust Trail. *Lunar and Planetary Science, XXXIV*, 2056.pdf.
- Lowry, S.C., Fitzsimmons, A., Collander-Brown, S., 2003. CCD Photometry of Distant Comets III: Ensemble Properties of Jupiter Family Comets, *Astron. and Astrophys.*, 397, pp. 329-343.
- Lowry, S.C., Fitzsimmons, A., 2005. William Herschel Telescope Observations of Distant Comets. *MNRAS* 358, 641-650.
- Meech, K.J., Newburn, R.L., 1998. Observations and Modeling of 81P/Wild 2, DPS Meeting 1998, Session 42. Meech, K.J., 2000. Cometary Origins and Evolution, p. 207-215. In "A New Era in Bioastronomy", ASP Conference Series, Vol. 213, 2000, G. Lemarchand and K. Meech, Eds.
- Meech, K.J., A'Hearn, M.F.A., McFadden, L., Belton, M.J.S., Delamere, A., Kissel, J., Klassen, K., Yeomans, D., Melosh, J., Schultz, P., Sunshine, J., Veverka, J., 2000. Deep Impact - Exploring the Interior of a Comet, 235-242, in "A New Era in Bioastronomy", Lemarchand, G., and Meech, K., Editors, ASP Conference Series, Vol. 213.
- Meech, K. J., Hainut, O.R., Marsden, B. G., 2004. Comet nucleus size distribution from HST and Keck telescopes. *Icarus*, 170, 463-491.
- Morris, C. S., Hanner, M. S., 1993. The Infrared light curve of periodic comet Halley 1986 III and its relationship to the visual light curve and C2, and water production rates. *An. J.*, 105, 1537-1546.
- Mueller, B.E.A., 1992, CCD-Photometry of Comets at Large Heliocentric Distances, *ACM* 1991, pp. 425-428.

- Mueller, B.E.A., Samarasinha, N.H., 2002. Visible Light Curve of Comet 19P/Borrelly, Earth, Moon and Planets, 90, p.463-471.
- Neslusan, L., 2003. Observed sizes of cometary nuclei. Contrib. Astron. Obs. Skalnaté Pleso, 33, 5-20.
- O Ceallaigh, D.P.O., Fitzsimmons, A., Williams, I.P., 1995. CCD Photometry of Comet 109P/Swift-Tuttle, Astron. and Astrophys., 297, L17-L20.
- Schleicher, D.G., Lederer, S.M., Millis, R.L., Farnham, T.L., 1997. Photometric Behavior of Comet Hale-Bopp (C/1995 O1) Before Perihelion. Science 275, 1913-1915.
- Schleicher, D.G., Osip, D. J., 2002. Long- and Short-Term Photometric Behavior of Comet Haykutake (1996 B2). Icarus, 159, 210-233.
- Scotti, J., 1995, Comet Nuclear Magnitudes, DPS Meeting, Session 43, BAAS, 26, p. 185.
- Scotti, J.V., (2001), Periodic Comet Extreme Observations, web Site, <http://pirlwww.lpl.arizona.edu/~jscotti/comets.html>
- Sekanina, Z., 1976. A Continuing Controversy: Has the Cometary Nucleus Been Resolved?, p. 537-585, in "The Study of Comets", Part 2, Donn, B., umma, M., Jackson, W., A'Hearn, M.A., Harrington, R., Editors, NASA SP-393.
- Sekanina, Z., 1985. Light Variations of Periodic Comet Halley Beyond 7 AU, Astron. Astrophys., 148, p. 299-308.
- Sekanina, Z., 1998. Nucleus of comet IRAS-Araki-Alcock (1983 VII). An. J., 1876-1894.
- Sekanina, Z., 2003. A Model for Comet 81P/Wild 2, J. Of Geophy. Research, 108, No. E10, 2-14.
- Stansberry, J.A., VanCleve, J., Reach, W.T., Cruikshank, D.P., Emery, J.P., Fernandez, Y.R., Meadows, V.S., Su, K.Y.L., Misselt, K., Rieke, G.H., Young, E.T., Werner, M.W., Engelbracht, C.W., Gordon, K.D., Hines, D.C., Kelly, D.M., Morrison, J.E., Muserolle, J., 2004. Spitzer observations of the dust coma and nucleus of 29P/Schwassmann-Wachmann 1, Ap. J., 154, 463-473.
- Snodgrass, C., Lowry, S.C., Fitzsimmons, A., 2006. Photometry of cometary nuclei: rotation rates, colours and a comparison with Kuiper Belt Objects. MNRAS, 373, 1590-1602.
- Tancredi, G., Fernandez, J.A., Rickman, H., Licandro, J., 2000. A Catalog of observed nuclear magnitudes of Jupiter Family Comets, Astron. Astrophys. Suppl. Ser., 146, 73-90.
- Tancredi, G., Fernandez, J.A., Rickman, H., Licandro, J., 2006. Nuclear magnitudes and the size distribution of Jupiter family comets. Icarus, 182, 527-549.
- Tsumura, M., 2006. <http://park10.wakwak.com/%7etsumura/>
- Yabushita, S., Wada, K., 1988. Radioactive Heating and Layered Structure of Cometary Nuclei, EMP, 40, p. 303-313.
- Vsekhsvyatskii, S. K., 1964. Physical characteristics of Comets. NASA TT F-80, OTS 62-11031.

Table 1. Comets with power laws at turn on.

| Comet     | P-AGE (cy) | Slope $n_{ON}$ |
|-----------|------------|----------------|
| C/1995 O1 | 1.8        | 10.30          |
| 1P        | 7          | 8.92           |
| 81P       | 13         | 10.43          |
| 19P       | 14         | 12.42          |
| 21P       | 20         | 9.09           |
| 9P        | 21         | 7.70           |

Table 2. Comets with a brake point in the power law.

| Comet     | P-AGE[cy] | $R_{BP}$ [AU] | $m_{BP}$ |
|-----------|-----------|---------------|----------|
| C/1995 O1 | 1.8       | -6.3          | 4.6      |
| 1P        | 7.2       | -1.70         | 5.6      |
| 81P       | 13        | -1.9          | 10.0     |
| 21P       | 20        | -1.58         | 10.6     |
| 9P        | 21        | - 2.08        | 13.8     |

Table 3. Look alike comets

| Comet                       | P-AGE | P-AGE | Comet                       |
|-----------------------------|-------|-------|-----------------------------|
| 1P/Halley                   | 7     | 1.8   | C/1995 O1 Hale Bopp         |
| 19P/Borrelly                | 14    | 102   | C/2001 OG108 LONEOS         |
| 21P/Giacobini-Zinner        | 20    | 13    | 81P/Wild 2                  |
| 26P/Grigg-Skjellerup        | 89    | 100   | 28P/Neujmin 1               |
| 28P/Neujmin 1               | 100   | 76    | C/1983 H1 IRAS-Araki-Alcock |
| C/1983 H1 IRAS-Araki-Alcock | 76    | 89    | 26P/Grigg-Skjellerup        |
| 39P/Oterma                  | 8     | 10    | 65P/Gunn                    |
| 107P/Wilson-Harrington      | 1370  | 1460  | 133P/Elst-Pizarro           |

Table 4. Basic photometric parameters deduced from the secular light curves in order of increasing P-AGE.

| Comet                  | Rank | R <sub>ON</sub><br>[AU] | R <sub>OFF</sub><br>[AU] | T <sub>ON</sub><br>[d] | T <sub>OFF</sub><br>[d] | P-AGE<br>[cy] | T-AGE<br>[cy] | m <sub>1</sub> | V <sub>N</sub> (1,1,0) | A <sub>SEC</sub> | LAG<br>[d] | q<br>[AU] | Q<br>[AU] | D <sub>EFFE</sub><br>[km] |
|------------------------|------|-------------------------|--------------------------|------------------------|-------------------------|---------------|---------------|----------------|------------------------|------------------|------------|-----------|-----------|---------------------------|
| 29P/SW 1               | 1    | <83                     | <240                     | ----                   | ----                    | 0.4           | ----          | -2.5           | 7-15                   | 10-17            | +1740      | 5.44      | 6.47      | 54                        |
| C/1995O1 H-Bopp        | 2    | -20.4                   | 43.7                     | -2670                  | 9000                    | 1.8           | 0.6           | -1.4           | 9-13.1                 | 10-14            | +45        | 0.91      | 369       | 17-96                     |
| C/1985XI Shoemaker     | 3    | ~11.8                   | 24.0                     | ----                   | ----                    | ~4            | ----          | 3.8            | <13.4                  | >9.6             | ----       | 2.70      | e=1       | <14                       |
| 1P/Halley              | 4    | -6.15                   | 12.6                     | -497                   | 1497                    | 7.1           | 4.2           | 3.4            | 14.13                  | 10.8             | +11.2      | 0.59      | 35.3      | 9.8                       |
| 39P/Oterma             | 5    | -7.7                    | 6.6                      | -2747                  | 3000                    | 9             | 1.4           | 3.0            | 14.52                  | 11.5             | 0          | 3.39      | 4.53      | 6.3                       |
| 65P/Gunn               | 6    | -7.4                    | 5.6                      | -1417                  | 1378                    | 10            | 3             | 4.0            | 14.7                   | 10.8             | +242       | 2.46      | 4.74      | 4.8                       |
| 81P/Wild 2             | 7    | -4.4                    | 5.8                      | -644                   | >864                    | 13            | <5            | 5.8            | 16.53                  | 10.7             | -13        | 1.58      | 5.30      | 3.9                       |
| 19P/Borrelly           | 8    | -2.9                    | >5                       | -266                   | >300                    | <14           | ----          | 4.0            | 16.0                   | 12.2             | +6         | 1.37      | 5.87      | 4.0                       |
| 73P/SW3C (2001)        | 9    | -5.2                    | 4.2                      | -950                   | 478                     | 18            | 7             | 8.3            | 17.1                   | 8.7              | ----       | 0.94      | 5.18      | 2.2                       |
| C/1996B2 Hyakutake     | 10   | -3.2                    | 3.52                     | -167                   | 189                     | 19            | 22            | 4.3            | 15.7                   | 11.5             | -6         | 0.23      | 1901      | 4.8                       |
| 101P/Chernykh          | 11   | -3.1                    | 4.9                      | ----                   | ----                    | 20            | ----          | 10.2           | 16.0                   | -----            | ----       | 2.36      | 9.24      | 5.0                       |
| 21P/G-Zinner           | 12   | -3.6                    | 5.4                      | -366                   | 660                     | 20            | 11            | 8.2            | 16.1                   | 7.9              | -10        | 1.03      | 6.0       | 3.1                       |
| 9P/Tempel 1            | 13   | -3.5                    | 4.2                      | -410                   | 659                     | 21            | 9             | 6.4            | 15.3                   | 8.9              | -10        | 1.50      | 4.74      | 5.5                       |
| 6P/D'Arrest            | 14   | -1.6                    | <3.4                     | -70                    | >250                    | <24           | <26           | ----           | 18.3                   | -----            | +46        | 1.35      | 5.62      | 1.6                       |
| 109P/Swift-Tuttle      | 15   | -2.7                    | 3.2                      | -123                   | 156                     | 30            | 40            | 3.8            | 11.9                   | 8.1              | +1         | 0.96      | 52        | 30                        |
| 67P/Churyumov-Geras    | 16   | -2.8                    | 4.0                      | -232                   | 408                     | 32            | 21            | 9.6            | 16.3                   | 6.7              | +33        | 1.30      | 5.73      | 5.2                       |
| 32P/Comas-Sola         | 17   | -4.1                    | 4.3                      | -324                   | 372                     | 33            | 19            | 7.7            | 15.6                   | 7.0              | ----       | 1.85      | 6.67      | 3.0                       |
| 85P/Boethin            | 18   | -1.8                    | 1.7                      | -107                   | 91                      | 49            | 54            | 5.9            | 14.3                   | 8.4              | -4         | 1.11      | 8.91      | 6.3                       |
| C/1983 J1 SSF          | 19   | -----                   | 1.5                      | ----                   | 60                      | 53            | 84            | 10.5           | 19.8                   | 9.0              | ----       | 0.47      | ----      | 0.7                       |
| 45P/Honda-Mrkos-P      | 20   | -1.5                    | 1.9                      | -70                    | 118                     | 55            | 64            | 12.0           | 19.5                   | 7.5              | +2         | 0.53      | 5.5       | 0.9                       |
| 2P/Encke 1858          | 21   | -2.2                    | 1.7                      | -126                   | 105                     | 58            | 61            | 9.1            | 15.5                   | 6.4              | -13        | 0.34      | 4.09      | 5.1                       |
| C/1983H1 IRAS-A-A      | 22   | -1.2                    | 1.6                      | -41                    | 70                      | 76            | 120           | 7.8            | 14.6                   | 6.8              | +19        | 0.99      | 199       | 8.6                       |
| 26P/G-Skjellerup       | 23   | -1.4                    | 1.8                      | -73                    | 132                     | 89            | 85            | 11.4           | 16.7                   | 5.2              | +14        | 0.99      | 4.93      | 3.0                       |
| 2P/Encke 2003          | 24   | -1.6                    | 1.5                      | -87                    | 94                      | 97            | 103           | 10.7           | 15.5                   | 4.8              | +6         | 0.34      | 4.09      | 5.1                       |
| 28P/Neujmin 1          | 25   | -2.1                    | 2.4                      | -115                   | 167                     | 100           | 100           | 9.6            | 12.8                   | 3.2              | +7         | 1.53      | 12.1      | 23                        |
| C/2001 OG108 LON       | 26   | -1.6                    | 1.6                      | -78                    | 96                      | 102           | 117           | 8.7            | 13.1                   | 4.4              | -5         | 0.99      | 25.6      | 15.8                      |
| 107P/Wilson-Harrington | 27   | +1.1                    | 1.4                      | +38                    | 74                      | 1370          | 720           | 12.9           | 16.3                   | 3.5              | +42        | 0.98      | 4.28      | 3.3                       |
| 133P/Elst-Pizarro      | 28   | +2.6                    | 2.8                      | +42                    | 233                     | 1460          | 80            | ----           | 16.0                   | 6.0              | +155       | 2.63      | 3.68      | 4.6                       |

## Figure Captions

Figure 1. Comet 103P/Hartley 2 imaged with the 1 m Schmidt telescope of the National Observatory of Venezuela, at f/3, on 2005, January 12<sup>th</sup>. Since large photometric apertures have to be used to extract the whole flux, the image has previously been cleaned of nearby stars using a cloning tool. The tail must be included in the measurement. Above: A normal stretching of the image shows that an aperture of radius 20 pixels is apparently enough to extract a total magnitude. Stretching refers to the maximum and minimum pixel intensity to display the image in the computer monitor. The standard stretching is selected by the computer, who does not know about preserving the flux. Thus the monitor displays a deceptively faint image. Right hand: A forced stretching reveals a much larger tail than expected. At least a 44 pixel radius is needed to extract a total magnitude. This has been called the *insufficient CCD aperture error* (Ferrín, 2005b), and manifest itself by producing measurements that lie much below the envelope of the observations. The comet had a magnitude of  $R= 16.66\pm 0.15$ , so it is easy to conclude that the effect is much larger for brighter comets.

Figure 2. Derivation of an infinite aperture magnitude. It can be seen how the calibration star and the comet increase in flux with increasing photometric apertures. The asymptotic value is the infinite aperture magnitude. Notice the huge aperture needed to extract the whole flux of the comet, much larger than typically used apertures. Notice also how the calibration star #14 converges rapidly

to its infinite aperture magnitude but still needs a 8 pixel radius to retrieve an IAM. If a comet of magnitude 16 needs an aperture of 2 arc minutes in diameter to extract the whole flux, then a brighter comet will need a much larger aperture. Usually and exponential decay fits the data.

Figure 3. Key to the log plot.

Figure 4. Key to the time plot.

Figure 5. Histogram of diameters of Jupiter Family comets. The distribution has been divided into bins to define size classes. It can be ascertained that most Jupiter Family comets have diameters less than 10 km.

Figure 6. Comparative effective diameters of comets. There are goliath comets that if they were to brake, they would give origin to thousands of small comets.